UNIVERSITY OF CALIFORNIA
Santa Barbara

Development of an Integrated Ground-Air-based Conservation Monitoring System for the Tejon Ranch Conservancy

A Group Project submitted in partial satisfaction of the requirements for the degree
of
Master of Environmental Science and Management
for the
Bren School of Environmental Science & Management

by

CHERYL BUBE
ELLIE CAMPBELL
AMANDA KELLEY
KALLI KILMER
JONATHAN PHAM

Committee in charge:
JAMES FREW

JUNE 2018

[This page intentionally left blank]

Development of an Integrated Ground-Air-based Conservation Monitoring System for the Tejon Ranch Conservancy

As authors of this Group Project report, we are proud to archive this report on the Bren School's website such that the results of our research are available for all to read. Our signatures on the document signify our joint responsibility to fulfill the archiving standards set by the Bren School of Environmental Science & Management.

_____
Cheryl Bube

_____
Ellie Campbell

_____
Amanda Kelley

_____
Kalli Kilmer

_____
Jonathan Pham

The mission of the Bren School of Environmental Science & Management is to produce professionals with unrivaled training in environmental science and management who will devote their unique skills to the diagnosis, assessment, mitigation, prevention, and remedy of the environmental problems of today and the future. A guiding principal of the School is that the analysis of environmental problems requires quantitative training in more than on discipline and an awareness of the physical, biological, social, political, and economic consequences that arise from scientific or technological decisions.

The Group Project is required of all students in the Master's of Environmental Science and Management (MESM) Program. It is a three-quarter activity in which small groups of students conduct focused, interdisciplinary research on the scientific, management, and policy dimensions of a specific environmental issue. This Final Group Project Report is authored by MESM students and has been reviewed and approved by:

_____
James Frew PhD., Faculty Advisor
March 2018

[This page left intentionally blank]

Acknowledgements

We would like to extend our sincerest gratitude towards the following individuals and organizations for their guidance and support throughout the duration of this project:

James Frew, PhD – Faculty Advisor, UCSB Bren School of Environmental Science and Management
Laura Pavliscak, MS – Client & Stewardship Manager, Tejon Ranch Conservancy
Michael White, PhD - Founding Science Director, Tejon Ranch Conservancy
Ben Teton - Biologist, Tejon Ranch Conservancy
Ashley Larson, PhD – UCSB Bren School of Environmental Science and Management
David Theobald, PhD – Colorado State University School of Global Environmental Sustainability
Mark Dufau – Director of Sales: Commercial, AeroVironment, Inc.
Todd White – Director of Flight Operations, RoboHawk Aerial Video & Imaging
Tom Dudley, PhD – Principal Investigator, Riparian Invasion Research Laboratory (RIVRLab), Marine Science Institute, UCSB
Nicole Norelli – Coordinator, California Alliance for Tamarisk Biocontrol, RIVRLab
Susan Mazer, PhD – Director, California Phenology Project

With additional thanks to:
Andrew Brooks PhD – Director, Carpinteria Salt Marsh, UC Natural Reserve System
Kyle Cavenough PhD – Assistant Professor, Geography, UCLA
Pranav Maroli – UCSB
Alexander Mikhailovsky, PhD - UCSB
Eduardo Romero – Marine Science Institute, UCSB
Arthur Sylvester PhD – Faculty Emeritus, UCSB
Sharad Shankar, PhD Candidate – UCSB

Table of Contents

List of Tables

List of Figures

Appendix Items

Appendix 1. Current UAV systems and specifications.
Appendix 2. Publically accessible databases available online that house different types of spectral and spatial data.
Appendix 3. NDVI cell grouping layer: ArcGIS ModelBuilder workflow.
Appendix 4. NDVI layer to NIR: ArcGIS ModelBuilder workflow.
Appendix 5. Images and descriptions of the plants chosen for classification training data.
Appendix 6. Twenty-five texture features calculated for each of the five grey-level bands.
Appendix 7. Details on the R "radiomics" package and R-ArcGIS bridge.
Appendix 8. R scripts for texture feature calculation and analysis.
Appendix 9. Texture analysis workflow.
Appendix 10. Inputs into the cost benefit analysis.
Appendix 11. Discriminant analysis model summary.
Appendix 12. Further applications of UAS technology.
Appendix 13. Further examples of imaging methods.
Appendix 14. List of satellite and aerial imagery sources and specifications.
Appendix 15. Traceability matrix.

Glossary of Terms

AGL (Altitude Above Ground Level): the height (in feet) above ground which a UAV flies over a land area locally.
AVIRIS (Airborne Visible/Infrared Imaging Spectrometer): a premier instrument in the realm of Earth Remote Sensing, AVIRIS is a unique optical sensor that delivers calibrated images of the upwelling spectral radiance.
ASTER (Advanced Spaceborne Thermal Emission and Reflection Radiometer): an instrument sensor resulting from a partnership between US and Japanese space programs, it sits aboard the Terra multinational satellite.
CASI-II (Compact Airborne Spectrographic Imager 2): a high spatial and spectral resolution remote sensing sensor that can produce digital geocoded imagery for map registrations, GIS integration, and generates multiple value-added information products from the same set of image data.
Drone: colloquial name for UAVs/UASs, the term is used in this project in reference to relatively small (<5 pounds), personal drones.
EO-1 Hyperion: a high-resolution hyperspectral imager, a USGS instrument
FAA (Federal Aviation Administration): a U.S. Department of Transportation Agency with the authority to regulate and oversee all aspects of American civil aviation.
Fixed Wing UAV: a drone model that has the appearance of an airplane, with rotors positioned on the wing tips.
Gimbal: an attachment used to add a camera to a drone. The function is to keep the camera stable for clear images.
Ground Truthing: used by remote sensing analysts to ensure that their image analysis is accurate; the process of going into the field to the actual places shown in the images to confirm that what they think they see on the image is actually true. This can be done before or after image collection.
KML (Keyhole Markup Language): a common file format for expressing geographic annotation and visualization within Internet-based, two-dimensional maps and three-dimensional Earth browsers.
Landsat (Land Remote-Sensing Satellite System): a joint NASA/USGS program, the Landsat series of satellites provides the longest temporal record of moderate resolution multispectral data of the Earth's surface on a global basis. "**TM**" refers to **Thematic Mapper**, one of the sensors aboard the satellites.
LOS (Line of Sight, or Visual Line of Sight): ability of pilots to see their drone during flight with the naked eye.
MaxEnt: a program for modeling species distributions from presence-only species records.

NDVI (Normalized Difference Vegetation Index): a graphical indicator that can be used to analyze remote sensing measurements to assess whether the target being observed contains live green vegetation or not.

NLCD (National Land Cover Dataset (2011)): the most recent national land cover product created by the Multi-Resolution Land Characteristics (MRLC) Consortium.

No Fly Zone: areas where flying a drone is restricted by government regulations. Areas where a drone could interfere with an airplane or record sensitive information make up most of these areas.

Part 107: Required in the US when operating a drone for commercial purposes. Refers to CFR Part 107 of the Federal Aviation Regulations for non-hobbyist unmanned aircraft operations, which covers a broad spectrum of commercial uses for drones weighing less than 55 pounds.

Payload: refers to anything extra that a drone is carrying (ex. an attached camera and gimbal). Also, refers to the amount of additional weight a drone is able to lift in addition to its own weight and batteries (ex. may include the combined weight of a drone plus the camera and gimbal attached to the drone).

Quadcopter: the most popular name for Small UAVs, which has 4 rotors positions on a horizontal plane like a helicopter.

Remote Sensing: the scanning of the earth by sensors on satellites or high-flying aircraft in order to obtain information about it.

Resolution: refers to spatial resolution, which describes how clearly detail can be seen in a picture. Measure in distance units per pixel (ex. inch/pixel, cm/pixel, or m/pixel).

Sensor: a device that records a remote sensing image, similar to a camera.

sUAS: small unmanned aircraft system

UAS (Unmanned Aircraft System): an all-encompassing term for everything that makes a drone/UAV operate (ground control station with pilot, communications, support equipment, etc.)

UAV (Unmanned Aerial Vehicle): an aircraft without a human pilot onboard – instead, the UAV is controlled from an operator on the ground. It is sometimes called a **drone.**

[This page left intentionally blank]

Abstract

The Tejon Ranch Conservancy helps manage over 100,000 acres of conservation easements located in Southern California at the intersection of four major ecological zones. The Conservancy's ability to monitor these easements is constrained by their small staff and limited budget. One of these monitoring targets is tamarisk, an invasive weed. Tamarisk infestations dramatically alter local landscapes, threatening native plants and animals, making it a management priority for the Conservancy. We explored how the Conservancy could use imagery from drones and satellites to expand their monitoring reach, using tamarisk as a proof of concept. We assessed the usefulness of drone and satellite imagery to identify invasive plant species to more effectively mobilize the Conservancy's limited weed management resources. We reviewed the capabilities of these technologies, completed a series of drone test flights over the property, developed image classification models to identify different weed species in ArcGIS, and identified areas susceptible to tamarisk invasion using the MaxEnt species distribution model. The results of these analyses were synthesized into an iterative monitoring framework. A cost benefit analysis of investment options in drone technology revealed that it is practical and effective for the Conservancy to purchase and operate a drone for monitoring purposes.

Executive Summary

The Tejon Ranch Conservancy is the management body for over 100,000 acres of conservation easements owned by the Tejon Ranch Company. The Conservancy aims to develop stewardship practices to maintain and restore the ecosystems that cover the Ranch, and expand understanding of the Ranch's unique and extraordinary natural resources. Tejon Ranch contains a diverse range of plants and animals due to its unique location at the convergence of four major ecological regions (Sierra Nevada, Mojave Desert, Great Central Valley, and Southwestern California), and is a critical wildlife corridor for several listed endangered species.

The Conservancy is responsible for monitoring expansive swaths of land, but its management resources are limited. Our research assesses if and how the addition of predictive modeling and high-resolution landscape mapping using unmanned aerial vehicles (UAVs or drones) and/or remote sensing would help the Conservancy make better use of its limited resources. We provide a cost-benefit analysis of these new technologies as compared to a baseline of the Conservancy's traditional management practices. One of the Conservancy's priorities is the management of invasive plant species. Our project focuses on weed management, the riparian weed Tamarisk *(Tamarix spp.)* in particular, as a proof of concept for enhancing conservation activities using an air-ground-based monitoring system.

We completed an initial literature review to assess the usefulness and cost effectiveness of different remote sensing and UAV technologies. We began with satellite imagery and tabulated different sources of satellite imagery with information about their temporal, spatial, and spectral resolution, operational lifetime, spatial accuracy, online community and support, and access. We systematically matched imagery sources to particular conservation questions or objectives, which we achieved through the creation of a Traceability Matrix. The Matrix matches conservation questions to useful or necessary sources of imagery, contingent on the specifications of each question. Regarding invasive plant species, a number of studies indicate Landsat data can successfully detect established tamarisk at larger spatial scales and in conjunction with spatial subsetting techniques. However, resolution of satellite sources is not fine enough for early-stage detection.

Because early-stage detection is critical to weed mitigation, we moved on to consider UAV or "drone" imagery, as it provides resolution on a much finer scale. Because Tejon Ranch is such a massive property, and using drones to attempt to image the entire Ranch would be an unwieldly process, we also considered it necessary to strategically identify land parcels that

would be good candidates for drone flights. To do this, we used MaxEnt, a species distribution model, to determine potential areas of invasive plant species occurrence at the Tejon Ranch Conservancy. MaxEnt uses presence data and environmental variables to predict species occurrence across a landscape. Presence data for plant species was sourced from the 2016 Incidental Weed Encounter Data provided by the TRC staff. We used tamarisk presence data in conjunction with nine environmental layers in MaxEnt 3.3.3. Our results show that Tamarisk probability of occurrence is highest along major streams (Fig. 15). Predictions of Tamarisk occurrence were fairly accurate with an area under the curve (AUC) of 0.989. Major streams had the largest contribution followed by soil type. All other variables had low (<5%) contribution. The areas identified by MaxEnt are those most susceptible to invasion, and are therefore priority site for drone flights to ensure rapid mitigation. One of those sites was Caliente Creek, where we identified a 40-acre field site called Panofsky to conduct test flights.

To determine if UAV imagery could be used to identify targeted locations of invasive weeds to the species level, ground truthing was conducted at the 40-acre Panofsky Field site prior to UAV flights. We performed a preliminary ground truth survey to identify and geotag common invasive and native plant species present throughout the Panofsky parcel. Before each drone flight, we placed cardboard arrow signs next to the target plants to assist with later locating the training areas in the drone imagery. After the geo-referenced stitched maps were created from the UAV imagery, we matched the ground truth data to the individual plant targets in the imagery.

Drone flights were performed on two separate flight days about one month apart at Panofsky Field. The first flight was conducted by RoboHawk Aerial Video & Photography on September 11, 2017, and the second by AeroVironment on October 12, 2017. RoboHawk Aerial Video & Photography was able to map Panofsky Field at multiple elevations (120 and 200 feet AGL) using a DJI Phantom 4 Advanced. Flight durations ranged from 40 minutes for the 120-foot AGL flight, to 1.5 hours for the 200-foot AGL flight to map Panofsky with three and four battery swaps, respectively. Over 1000 individual still images were captured from the Phantom 4 flights and stitched into a mosaic map. AeroVironment used their precision agriculture drone platform, the Quantix, to map Panofsky Field in less than 10 minutes at an altitude of 360 feet AGL and generate preview mosaics in the field.

After the imagery was acquired, we attempted two methods of image classification to automate the identification of plant species: pixel-based maximum likelihood classification, and object-based discriminant analysis. For the pixel-based classification, a composite 4-band image (NIR+RGB) was generated from the drone imagery for use as input into a supervised classification. Using the ArcGIS Maximum Likelihood Classification tool, defined training

samples were selected from ground truthed plant patches to serve as confirmed positive matches. Based on the spectral properties within the defined patches, the tool classified individual pixels to one of four classes (tamarisk, short pod mustard, tree of heaven, and a general oaks class). With a conservative reject fraction of 0.25, the software was successfully able to identify individual oaks and short pod mustard patches, but was generous in its over classification of tamarisk and tree of heaven throughout all regions of the parcel.

For the object-based classification, we used an R statistical package called radiomics and ArcGIS ModelBuilder to develop a method to calculate 25 different texture features within the drone imagery. Imagery from both drone test flights was used, with 1 cm resolution RGB imagery from the first and 5 cm resolution NIR from the second. Discriminant analysis, a statistical technique for identifying patterns characterizing classes, was used to classify the image from the derived texture features. In test the methods capabilities in distinguishing invasive tree of heaven in the test imagery, we found that this method was unable to distinguish tree of heaven with our limited groundtruth dataset to a useful level of accuracy. The model had a low percentage of false negatives, as only 9 of 60 presence points were classified by the model as "absence" points. However, the classification of tree of heaven had a training error of 0.15 and with 51 true positive and 26 false positives, and the model's precision was 66.2%. Despite the mixed results of our analyses, it is clear that the implementation of drone technologies can drastically increase data collection abilities but can be optimized for specific applications such as habitat monitoring and surveying.

Finally, A cost benefit analysis was completed to evaluate two potential management options that incorporate drone technology into the Conservancy's monitoring strategies: (1) the Conservancy purchases a drone and all related accessories and permitting or (2) the Conservancy contracts a drone service to conduct monitoring flights over the property. Information about the costs for each option was collected and simulated over a five-year period. We chose this short period in recognition of the rapid evolution of drone technology, as the cost of commercially available drones and drone-related services will decrease over time. The benefits of drone technology were quantified in terms of time savings, hinging on the assumptions that drone technology would maintain the same accuracy as a field survey in identifying invasive plants. Using information about how much time the Conservancy spends on weed monitoring, it was determined that implementing drones would yield discounted time savings of $16,524.64 over five years. For option 1, this translated into a benefit-cost ratio of 1.15, with the overall costs for the five years amounting to about $14,325. Option 2 yielded dramatically different results, as costs for contracting a drone service to replicate our trial flight once a month over five years amounted to over $100,000. This resulted in a benefit-cost ratio of 0.15. Option 1 is thusly far more favorable than option

2, but is only slightly more favorable than the status quo of current monitoring strategies. However, this CBA was limited to the benefits of using drones for monitoring weeds, so it is reasonable to assume that if benefits were expanded to include all Conservancy activities, the overall benefits of a drone purchase would only increase while costs remain relatively static.

Our research confirmed that drones, if properly utilized, can be a useful tool to expand the monitoring reach of the Tejon Ranch Conservancy. However, Tejon Ranch is too large and variable in terrain to monitor in its entirety, multiple times per year, as would be desirable to detect invasive plant presence. Therefore, the Conservancy must be able to prioritize specific areas to target for drone surveys. Through our MaxEnt model, the Conservancy can identify highly susceptible areas to conduct flights. The presence data that would be gathered from these flights could then be used as inputs into new iterations of the MaxEnt workflow to more accurately predict future invasive plant dispersal risk. This creates a positive feedback loop in which the workflow is continually updated with environmental data and new presence data, and the overall monitoring framework becomes more robust and efficient. The Conservancy could also adapt this monitoring framework to include other conservation interests such as conifer mortality and endangered species monitoring. We believe that this framework may have potential applications for similarly resource-constrained organizations like the Conservancy, facilitating conservation activities despite financial limitations.

1. Introduction

1.1 Tejon Ranch Conservancy

The Tejon Ranch is the largest private landholding in California. At over 270,000 acres, this property, located near Lebec, California, is owned by the Tejon Ranch Company. In 2008, the Tejon Ranch Conservancy was established as the management body for 109,000 acres of conservation easements belonging to the Tejon Ranch Company (RWMP, 2013). This partnership between corporate and nonprofit entities has helped facilitate research, stewardship, and public access in conserved lands since its inception (RWMP, 2013). Conservancy-monitored lands consist of approximately 240,000 acres of varied landscapes including desert, steppe grasslands, mountainous conifer stands, and oak galleries. The Conservancy aims to develop stewardship practices to maintain and restore these Ranch ecosystems, and expand understanding of the Ranch's unique and extraordinary natural resources (RWMP, 2013). Tejon Ranch is of conservation interest due to its unique location at the convergence of four major ecological regions (Sierra Nevada, Mojave Desert, Great Central Valley, and Southwestern California) containing a diverse range of plants and animals (**Figure 1**). The Ranch is a critical wildlife corridor between the many protected lands in the area, from the Sierra Nevada to the Los Padres National Forest (RWMP, 2013). It supports habitats for several species listed under the Endangered Species Act including the California Condor and Bakersfield cactus (US Fish & Wildlife Service, 2017).

The Conservancy is responsible for monitoring expansive swaths of land, but in recent years has found itself low on resources with which to look after its properties. Our research assesses if and how the addition of predictive modeling and high-resolution landscape mapping using unmanned aerial vehicles (referred to hereafter as UAVs or drones) and/or remote sensing would help the Conservancy make better use of its limited resources. We provide a cost-benefit analysis of these new technologies as compared to a baseline of the Conservancy's traditional management practices outlined in the Ranch Wide Management Plan (RWMP). The RWMP is a blueprint for the Conservancy's management actions, with one priority being the management of invasive plant species. Our project focuses on weed management as a proof of concept for enhancing conservation activities using an air-ground-based monitoring system.

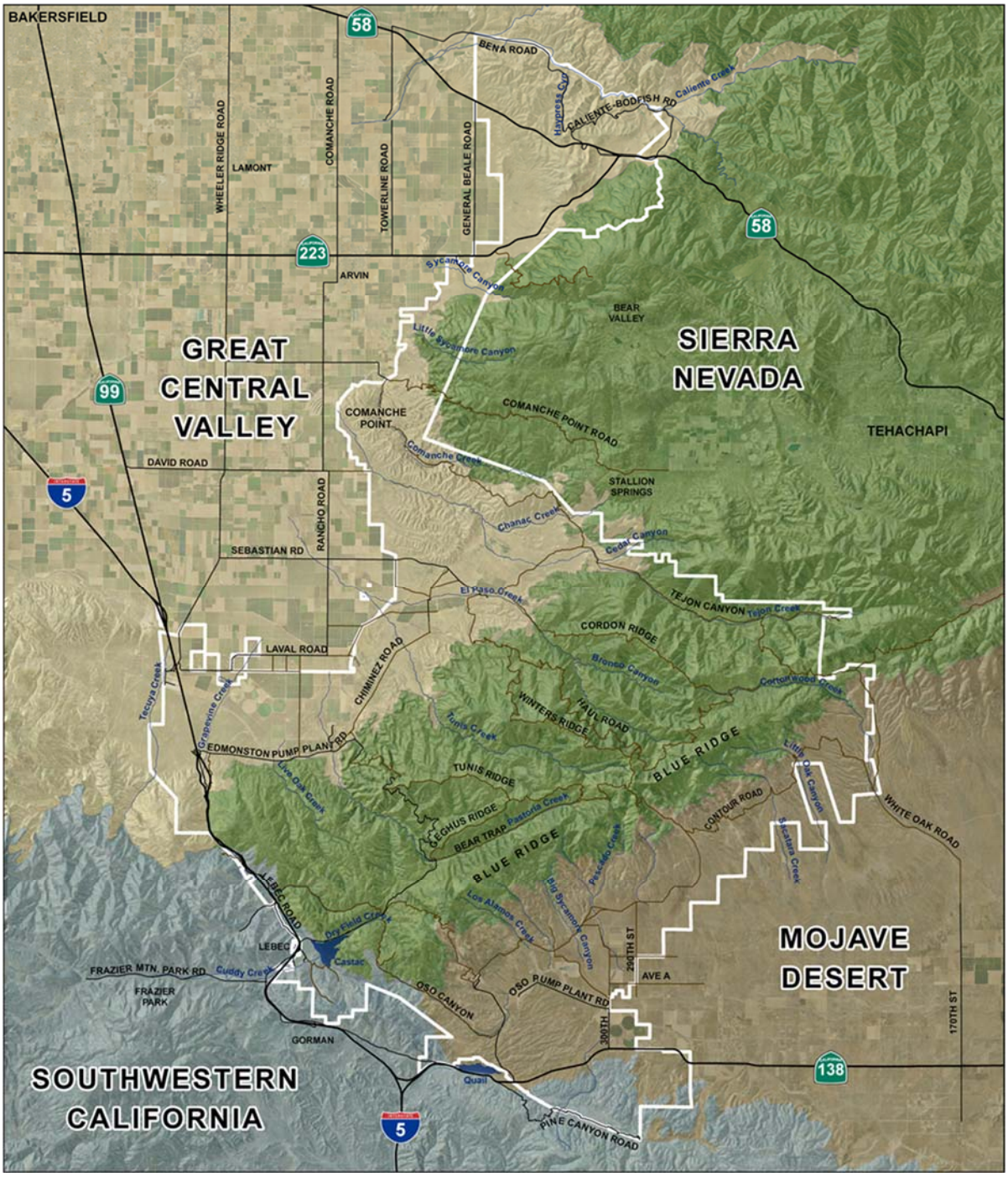

Figure 1. *A map of the four ecoregions that overlap within the bounds of Tejon Ranch. The Ranch boundaries are delineated in white.*

1.2 Project Objectives

The purpose of this project is to:

- Review current methods for air-ground-based monitoring. Determine what can be measured using drones, and what resources are required to analyze drone data. Compare the effectiveness of existing methods using open access spatial data such as Landsat and AVIRIS.
- Determine how these technologies can be used at the Tejon Ranch Conservancy to identify species and regions of interest, using the invasive weed tamarisk as a case study.
- Develop an integrated air-ground-based monitoring framework for the Tejon Ranch Conservancy based on the costs and benefits of drone and remote sensing technologies.

1.3 Significance of the Project

These objectives support the Conservancy's efforts to better understand Tejon Ranch's rapidly changing ecosystem dynamics and more effectively steward the land in response to growing threats such as invasive plant species and climate change. An exploration in the modeling of plant distributions and its role in ecosystem monitoring can prove to be fruitful when managing reserves with limited field staff. On a large property with the scale of Tejon Ranch, early detection of invasive plant spread enables early mitigation. While the Conservancy complies with best management practices in regards to species-specific plant disposal, rapid detection can be achieved through the integration of monitoring and modeling technology. Our plan seeks to establish a framework for the union of such technologies in a conservation context that is both applicable for landscapes beyond Tejon Ranch and accessible for resource-constrained managers like the Conservancy.

2. Background

2.1 Vegetation & Ecosystem Management by Tejon Ranch Conservancy

Top-Priority Invasive Species on Tejon

Several invasive plant species are of particular concern to the Conservancy, including Sahara mustard, shortpod mustard, tree tobacco, yellow starthistle, and tamarisk (also known as saltcedar, *Tamarix ramosissima,* and *Tamarix parviflora*). According to the United States Department of Agriculture, invasive species are "plants, animals, or pathogens that are non-native (or alien) to the ecosystem under consideration and whose introduction causes or is likely to cause harm" (USDA, 2018). Invasive weed monitoring is critical to the goals of the Conservancy. The proliferation of invasive plants such as tamarisk can drain creeks and springs as it outcompetes native willows and cottonwoods in terms of water acquisition (Gaskin, 2003). Tamarisk typically grows in saline soils and can tolerate a maximum of 15,000 ppm of soluble salt. It is also capable of increasing soil salinity and can tolerate alkaline soil types, evident by the salt secretions that often encrust its leaves. Other negative impacts of tamarisk include increasing the frequency and intensity of fires (Busch, 1995; Busch and Smith, 1995; Ellis et al., 1998) due to the plant's vegetation structure and floods due to channel-narrowing (Blackburn et al., 1982).

Tamarisk Biology and Management

Tamarisk grows as an evergreen, deciduous shrub or small tree (Evangelista, 2009). Phenologically, these plants have slender branches, small scale-like leaves of grey-green, and bark that progresses from reddish brown and smooth when young, to bluish-purple with furrows and ridges when older (Dirr, 1997). When flowering, it can be easily identified by its dense masses of characteristic small, pink flowers, aiding in its dispersal as an invasive plant species that is present at several locations on Tejon Ranch.

Tamarisk eradication methods often include manual stem cutting paired with direct application of herbicide to the stump. Our research group was able to participate in bio-control efforts on the ranch led by UCSB's RIVR (Riparian InVasion Research) lab using tamarisk beetles (*Diorhabda carinulata).* This invasive plant as well as other invasive plant species such as yellow starthistle thrives in such disturbed habitats. Yellow starthistle (*Centaurea solstitialis*) is highly vectorized via roads (AMNH). It is an aggressive invader that can rapidly convert landscapes into monocultures by outcompeting most other vegetation

including native plant species. Late in the season, it turns from green to dry skeletons of yellow starthistle. In effect, this can exacerbate the buildup of dry vegetative fuel load and create fuel for late-summer wildfires (DiTomaso et al., 2006).

Current Management Strategies for Invasive Plant Species

Currently, invasive plant species, such as tamarisk, Sahara mustard, shortpod mustard, tree tobacco and others, are identified and located on the Ranch using time-intensive, infrequent, or costly methods including incidental on-the-ground observations, helicopter aerial surveys, or contracted botanist plant surveys. The Conservancy complies with best management practices in regards to species-specific plant disposal.

2.2 Integrating Distribution Models and Detailed Monitoring for Exotic Plant Management

The MaxEnt Model

MaxEnt is a software model that uses presence-only data and environmental variables to produce an estimated species distribution in a defined area (Merow et al., 2013), by creating a distribution of maximum entropy using a set of constraints including climate, topography, and vegetation (Hoffman et al., 2008). A study compared MaxEnt to 16 other species distribution models and concluded that MaxEnt was most accurate (Hoffman et al., 2008). To increase the accuracy of MaxEnt, more presence data can be included in the model. Models with at least 400 presence data points have been shown to have the most accurate results, but in some instances models with 100 presence data points have performed comparatively (Phillips et al., 2004).

Modeling Plant Species Distribution with MaxEnt

There are well over 1000 published studies that have used MaxEnt to predictively model species distribution (Merow et al., 2013), one of which used MaxEnt to predict the distribution of five invasive species including tamarisk along the North Platte River in Nebraska (Hoffman et al., 2008). The environmental variables used by Hoffman et al. included WorldClim climate data, elevation, slope, aspect, vegetation, soil type, and distance from roads, streams, and other human impacts. Hoffman et al. concluded that MaxEnt accurately predicted the distribution of four out of the five species and speculated that the fifth species was not predicted correctly because of sampling error.

2.3. Satellite Imagery for Environmental Monitoring

Vegetation Mapping for Conservation Planning and Management

Technological progress in image resolution and sensor development has greatly improved the ability to distinguish canopy structure, and physiology and phenology of vegetation from remotely sensed imagery. Vegetation mapping via image processing techniques applied to remotely sensed imagery is a rapidly evolving field with many high-potential applications for conservation planning and management (Ustin & Gamon, 2010; Müllerová et al., 2013; Joshi et al., 2004; Xie et al., 2008; Hestir et al., 2008; Ustin et al., 2004). Satellite imagery has been used to detect stress and mortality in coniferous forests (Bright et al., 2013; Eitel, 2011; Meddens et al., 2013; Ferrell et al., 1993; Hicke & Logan, 2009; Ortiz et al., 2013), map vegetation at landscape scales (Roth et al., 2015; Rogan et al., 2002; Dye et al., 2016; Xie et al., 2008; Van de Ven & Weiss, 2001; Dabrowska-Zielinska et al., 2014), and aid in detection of invasive plants (Sankey et al., 2014; Hestir et al., 2008; He et al., 2011; Narumalani et al., 2009; Lawes & Wallace, 2008; Ghulam et al., 2013; Skowronek et al., 2017).

Detection of Tamarisk from Satellite and Aerial Imagery

The detection and mapping of two tamarisk species of high concern to the Tejon Ranch Conservancy, *Tamarix ramosissima* and *T. parviflora*, have been extensively studied (West et al., 2016; Meng et al., 2012; Evangelista et al., 2009; Hamada et al., 2007; Everitt et al., 1990). Detection algorithms can use single-date imagery or time series, as well as additional environmental data/variables. Everitt and Deloach recommend that single-date aerial assessments of large infestations of tamarisk be done in the late fall or early winter and in mid-January for smaller populations after foliage changes color but before it drops (Everitt & Deloach, 1990). West and her team used eight months of Landsat imagery as inputs to five species distribution models to detect tamarisk distributions based on phenological differences from nearby vegetation (West et al., 2016). They recommend topography, climate, and soil layers be included when predicting suitable habitat but that a limited number of these environmental and climate layers be used when modeling current distribution (West et al., 2016).

Landsat TM data has been used to effectively monitor tamarisk defoliation, though other types of disturbance or defoliation in the area can distort the signal (Meng et al., 2013; Hurley, 2004). Many studies will subset the area prior to using detection algorithms to help reduce these false positive errors. For example, one study used the National Land Cover Dataset

(NLCD) class 90 (woody wetland) to subset a study area likely to contain tamarisk, and then applied a disturbance index to detected defoliation (Meng et al., 2013).

Limitations of Satellite Imagery in Environmental Monitoring Applications

While its usefulness is illustrated by these studies, there are still significant limitations to using satellite imagery for environmental management. (1) Available and/or affordable imagery may not be of high enough spatial, temporal, and/or spectral resolution to resolve certain targets, especially in the presence of confounding environmental variables; (2) designing and calibrating methods to extract specific information may require a high level of expertise in remote sensing methodology and/or ecology of target species; (3) depending on methods and imagery used, large-scale monitoring may be very computationally intensive, and (4) the methods must be robust to slight variations in resolution and calibration of sensors to be reusable over time.

The results from our literature review of satellite detection applications for the Conservancy are condensed into a Traceability Matrix (appx. 15) that matches conservation questions to useful or necessary sources of imagery, contingent on the specifications required to analyze imagery with accuracy.

2.4 Unmanned Aerial Systems Imagery for Environmental Monitoring

UASs for Environmental Monitoring

For decades, governments have been developing UAS technology (Unmanned Aerial Systems or drones), typically for military specific uses such as intelligence gathering. Now, private UAS manufacturers are providing consumers with smaller, ready-to-fly drones at commercially affordable prices (<$1000), with low operating costs, and the added benefit of increased flight flexibility to immediately capture rapidly changing ecological processes or patterns (DJ2I; Yuneec; Rango et al., 2009). These remotely operated platforms can be outfitted with imaging sensors capable of collecting high-resolution imagery in thermal and near infrared wavelengths as well as the visible range of the electromagnetic spectrum (Michez et al., 2016; Gonzalez et al., 2016). In this report we refer to UAVs, UASs, and drones interchangeably.

Environmental monitoring through the use of drones can avoid common remote sensing issues such as cloud cover, and allow researchers or managers to identify vegetation species more confidently (Anderson and Gaston, 2013; Dehaan et al., 2012). Personal drones allow for more flexible timing of flights and thus can provide more valuable time-scale survey data than satellite data, which may not be as useful without significant, time-consuming image

processing. This can be critically important to monitoring and managing invasive plant surges in response to precipitation or disturbance events (Davies and Sheley, 2007).

Drones have demonstrated high potential for conservation applications in a variety of fields, including thermally identifying Koala nests in Queensland, Australia (Gonzalez et al., 2016), assessing habitat vegetation cover types and habitat quality for the Sage Grouse in Idaho (Breckenridge et al., 2011), estimating South Korean coniferous tree coverage area (Ivosevic et al., 2017), and discriminating invasive thistle plants from surrounding vegetative cover in Greece (Tamouridou at al., 2017). This technology can also be useful for easement compliance monitoring because users can pre-program geographically confined flight paths to map parcel areas or boundaries.

Unmanned Aerial Vehicle (UAV) Design

Drone design can generally be divided into two categories: (1) Multi-Rotor and (2) Fixed Wing configurations. Multi-rotor designs are typically less expensive and, unlike fixed winged designs, they can halt forward flight, hover, and rotate the camera to focus on or follow specific targets. Multi-rotor drones like the DJI Phantom 4 benefit from vertical take-off and landing and come with obstacle avoidance, which is useful in non-open environments. Fixed winged platforms fly in the same manner as traditional airplanes with fixed imaging cameras in the plane's "belly" facing towards ground targets. This format can cover more land area per flight when compared to multi-rotor platforms, but imagery can be subject to motion blur if the sensor is not sufficiently stabilized or synchronized to the flight speed (Breckenridge et al., 2011). Some fixed wing platforms need a second operator to launch the drone. Depending on the design, landing either requires an open area for a controlled crash or the drone can be caught by a second operator. Another drone model is the hybrid fixed wing platform, which has vertical takeoff and landing features and transitions into horizontal flight once it reaches a certain height above ground level. See **Appendix 1** for a comparison table of current consumer drone platforms.

Federal Regulation of Commercial Drone Use

In 2016, the Federal Aviation Administration (FAA) in collaboration with the Department of Transportation (DOT) published Part 107 of the FAA Regulations, which specifies the certifications required for legal and safe commercial UAS operation. A Part 107 permit is required for any individual who is using a drone for non-recreational purposes, such as crop monitoring, research, bridge inspections, rescue operations, or wildlife nesting area evaluations (FAA, Part 107). Permits can be obtained by passing an aeronautical knowledge test at an FAA-approved testing center. Drones may be flown only in the daytime, at a

maximum altitude of 400 feet above ground level, while always remaining within visual line of sight of the operator without optic aids (FAA, Part 107). The visual line of site requirement is a major limiting factor when surveying large parcels of land but is expected to be relaxed to permit optical aids in future revisions of UAS regulations. Other restrictions include maintaining distance from airports and avoiding high wind conditions. These regulations are in place to ensure safe operation of small aircraft platforms because they often share airspace with larger aircraft.

2.5 Image Processing for Satellite and UAS Imagery

Image Processing for Classification of Vegetation

The multistep process of obtaining useful information from remotely sensed imagery includes (1) imagery selection, (2) preprocessing, and (3) classification (Xie et al., 2008). Image selection is based on spectral, spatial, and temporal resolution, which determine what information can be extracted from the imagery (Appx. 2). Depending on the imagery selected, preprocessing may consist of mosaicking or "stitching" multiple images, radiometric or atmospheric corrections, subsetting data to remove bad spectral bands or images with cloud cover, or dimension reduction like Principle Component Analysis or Minimum Noise Fraction.

Image classification algorithms are either object-based or pixel-based. Pixel-based algorithms can be further categorized into either supervised or unsupervised classifications. Supervised classifications include maximum likelihood, random tree, and support vector machine in ArcGIS, and minimum distance and spectral angle mapper in ENVI, and require representative ground truth data points as training sites. Iso-Cluster in ArcGIS is an unsupervised classification algorithm, which statistically forms a specified number of unique classes without training sites. Pixel-based classification differentiates between categories or types of things in an image by statistically grouping pixels together based on their relative magnitudes in spectral bands (specific ranges of the electromagnetic spectrum measured by the sensor; e.g. a red band might sense wavelengths between 650 and 750 nanometers).

Object-Based Image Analysis and Texture

Object-based methods delineate objects in an image by grouping neighboring pixels with similar spectral characteristics (Schiewe, 2002; Ryherd & Woodcock, 1996). As spatial resolution has increased, objects of interest can be resolved in more detail, so object-based image analysis has emerged as a way to extract additional useful information. This is especially true of UAV-acquired data as it can have spatial resolution on the order of centimeters (Blaschke, 2010; Laliberte & Rango, 2008; Feng et al., 2015). Furthermore, high

spatial resolution can increase spectral within-field variability, which can diminish accuracy of pixel-based classifiers, making object-based analysis a particularly effective strategy for UAV-acquired imagery (Schiewe, 2002).

Texture features – spatial patterns in an image, with properties like coarseness, contrast, directionality, line-likeness, and regularity – have been considered as a way to compensate for the lower spectral resolution (most UAV sensors have only a few spectral bands) of UAV imagery (Ryherd & Woodcock, 1996; Laliberte & Rango, 2008). For example, texture features increased classification accuracy of invasive *Fallopia japonica* – a species with characteristic texture, but usually occurring in small patches and with high degree of intermingling with other plants – when mapped with low-cost RGB+NIR orthophotos (Dorigo et al., 2012). Additional studies were limited to a few broader vegetation groups, though they also find texture is a valuable addition, especially mean, standard deviation, and entropy features (Laliberte & Rango, 2008; Feng et al., 2015; Szantoi et al., 2013). Object-based image analysis has also been used for semi-automatic detection of dead trees following bark beetle outbreaks, with methods able to detect dead trees at a finer scale than visual interpretation, even within smaller, isolated stands (Heurich et al., 2010).

UAS Image Processing

UAS survey flights collect hundreds of geo-referenced still images that must be stitched into a larger mosaic image to fully represent the surveyed area. With a capable computer and access to software such as Agisoft's PhotoScan or Pix4DMapper, conservationists and researchers can produce georeferenced mosaic maps suitable for management decisions (Pix4D) (Agisoft). However, this procedure is computationally demanding, to the extent that some UAS investigations may choose to outsource their image processing. Software platforms and services now exist that can help automate UAS survey flights and offer licenses for unlimited image mosaicking and geo-referencing in exchange for membership fees (DroneDeploy).

Limitations and Hurdles to UAS Image Analysis for Monitoring

Post-survey image analysis must be performed for imagery to be useful to conservation managers on a landscape scale. Fully utilizing the potential of UAS in their environmental monitoring protocol will require investment by the Tejon Ranch Conservancy in staff training for drone operation, but also software licenses and computing resources. Once these initial hurdles are cleared, UAS habitat surveys and image analysis can become the foundation for a replicable protocol that will provide robust time-scaled data.

3. Methods

3.1 Flights & Ground Truthing

Ground Truthing the Panofsky Field Site

To determine if UAV imagery could be used to identify targeted locations of invasive weeds to the species level, ground truthing was conducted at the Panofsky Field site prior to UAV flights. Panofsky Field is an approximately 40-acre field site located adjacent to the northern border of the Tejon Ranch property. A preliminary ground truth survey was performed to identify and geotag invasive and native plant species present throughout the Panofsky parcel using an Avenza Map (an iOS app) with approximately 5-10 m accuracy. Each target plant was then marked with an identification-numbered orange marker flag.

We chose our targets based on common species and invasive species of interest present at the site. Our goal was to identify individual plant species at various stages of phenology to create thorough representative libraries. We intentionally looked for and geotagged a wide representation of plant species of interest, in a diverse representation of different habitats within the site (i.e. creekbed, creek bank, grasslands, roadsides, vernal pools, wetland areas, etc.). Descriptive notes were also taken to assist with plant identification during image processing. Once identified, we collected additional defining characteristics such as diameter, percent greenness, flower presence and color, seed presence and relative abundance, proximity to other plants, and other identifying descriptors. A total of 67 individual plants were tagged and geo-referenced at Panofsky Field.

Before the flight, we replaced the marker flags with cardboard arrow signs next to the target plants to assist with locating the training areas in the drone imagery. Each sign was made from 10” x 18” light brown cardboard with a large, bold arrow painted in black matte spray-paint to minimize sunlight reflection in the UAV imagery. This signage method was based on a similar method from a 2017 study by Lu and He. To classify species in a heterogeneous grassland, Lu and He used unified white foam boards labeled with plot ID codes, which were affixed to the ground near each study plot to be visible in UAV-acquired imagery. After the geo-referenced stitched maps were created from the UAV imagery, we matched the ground truth data to the targets in the imagery (**Figure 2**). This process is described in section 3.2.

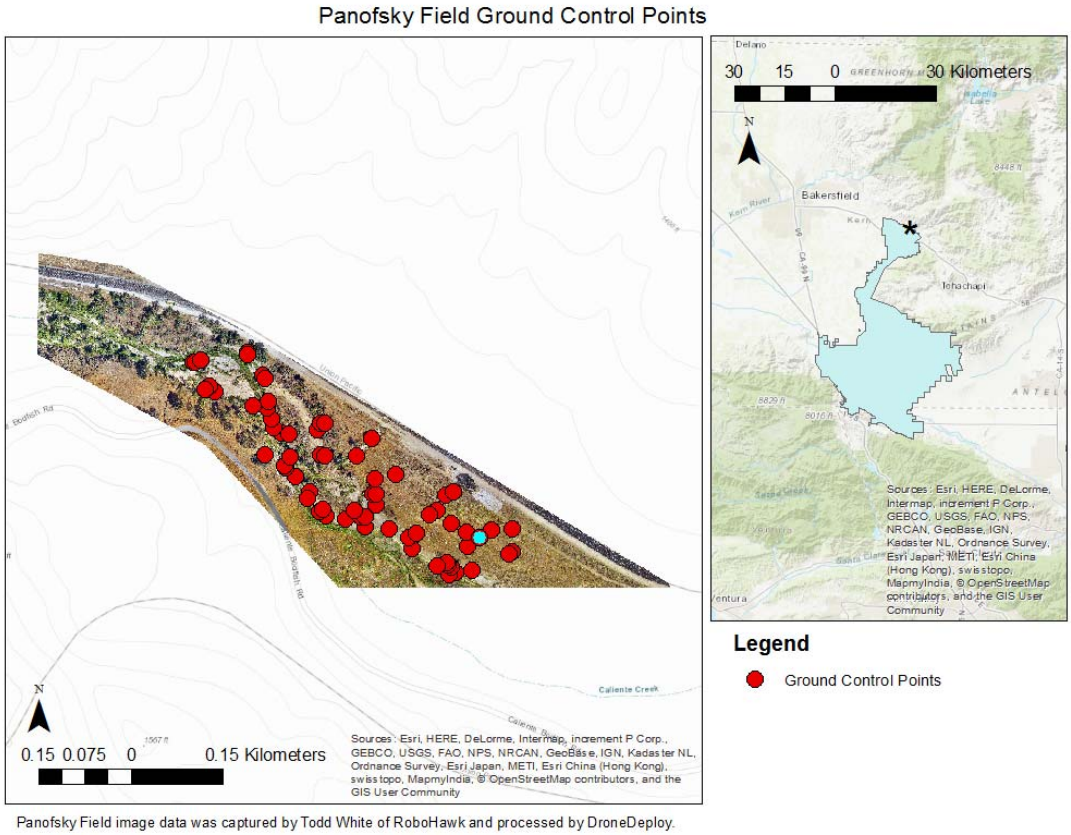

Figure 2. *Panofsky Field training areas. Map (left side of figure) of tamarisk training areas (red dots) at the Panofsky Field UAV test flight site. Inset map (right side of figure) indicates with a star the location of Panofsky Field along the northern border of the Tejon Ranch Conservancy.*

RoboHawk Flight

RoboHawk Aerial Video and Photography, a UAV consulting company, performed multiple surveys of Panofsky Field at varying altitudes using a DJI Phantom 4 UAV on September 11, 2017 (**Figure 3**). The Phantom 4 system is a commercially available quadcopter platform with vertical takeoff and omni-directional flight features. Two main flights were conducted: the first at 200' above ground level and the second at 120' above ground level (AGL). The first flight covered the entire plot (~40 acres) in approximately 39 minutes (9:30-10:09am) requiring one battery swap (two total batteries for entire flight). The second flight covered the entire plot in a total of 1 hour and 36 minutes (10:09-11:45 am) and required 3 battery swaps (4 total batteries for entire flight). Time-of-day is important to consider in order to minimize the influence of shadows and consistency for time-scale comparisons.

Figure 3. *RoboHawk's DJI Phantom 4 Advanced in flight over Panofsky Field.*

The drone's automated flight path was generated in the iOS application DroneDeploy from a KML file outlining the Panofsky Field parcel boundaries. Based on the boundaries of the area to be surveyed, the application will generate an overlapping "lawnmower" flight pattern to obtain the highest quality mosaic possible. The flights were programmed to have a front and side overlap of 75% using a 12-megapixel RGB (red, green, blue bands) camera. To offset the heavy computational demands of image mosaicking, all RoboHawk-collected imagery was uploaded to DroneDeploy's cloud service that processed and generated geo-referenced orthomosaic maps at resolutions of 5 cm/pixel (at 200' AGL) and 1 cm/pixel (at 120' AGL) from the 1000+ original JPEG images. Orthomosaics are composite images made of many individual still photos that also correct for distortion attributed to factors such as the earth's surface and camera lens distortion.

AeroVironment Flight

AeroVironment, Inc. (AV) used their new agriculture-specific platform, Quantix, to map Panofsky Field. AV is targeting Quantix at commercial agriculture usage with integrated sensors collecting 18 megapixel RGB and Near-Infrared data to inform vegetation health assays. The Quantix system is a unique fixed wing, forward flying design that can also takeoff and land vertically like a quadcopter system (**Figure 4**). The AV survey flight took place at Panofsky Field on Oct 12, 2017 and covered the entire plot in 9 minutes (10:24-10:33am) at a fixed altitude of 360' AGL. AV's Decision Support System's (DSS) software allows users to pre-program flight paths like DroneDeploy, but also allows users to obtain field-processed preview mosaics for preliminary analysis. DSS is similar to DroneDeploy in that flight paths are typically "lawnmower" patterns. The flight was programmed to have a side overlap of 70-75% while flying at a fixed altitude of 360' AGL to optimize image quality from the fixed aperture sensors. Processed outputs from this flight were georeferenced orthomosaics at resolutions of 2.5 cm/pixel.

Figure 4. *AeroVironment's Quantix drone in preparation for takeoff.*

3.2 Image Processing

We used two methods of image processing in attempts to discriminate tamarisk from other plant species of interest in the imagery acquired by the drone flights (**Figure 5**). Both methods are types of supervised classifications, as described in the background section. The first method described below is a pixel-based maximum likelihood classification, and the second is an object (i.e., polygon) based discriminant analysis classification. We chose to explore these two methods specifically because the computing tools that are required to complete them are easily accessible to the Conservancy, and can potentially be replicated by Conservancy staff should they choose to employ this technology.

Figure 5. *LEFT: The image of Panofsky Field captured by the DJI Phantom 4 Advanced; RIGHT: The same site captured by AeroVironment's Quantix.*

Classification: Pixel-based Maximum Likelihood Classification

Normalized Difference Vegetation Index (NDVI) is an indicator of vegetative health, based off reflectance of visible and near-infrared light. Living plants containing photosynthetically active chlorophyll absorb more visible light in the red and blue wavelengths, which contributes to their common green appearance. NDVI can provide the Conservancy with the ability to quantitatively monitor the efficacy of their biocontrol management efforts through seasonal flights measuring tamarisk dieback. Understanding that different plant species can have different amounts of relative chlorophyll at a given time, the differential absorbance from the varying plant species was used to inform our supervised classification.

Quantix output maps provided Red band data and NDVI data, but NIR bands are required to establish unique spectral signatures for each defined plant class. Thus, the NIR band must be recovered algebraically, by the process detailed in the following section.

NDVI Cell Grouping Layer Methods

In order to reduce the processing load on our computing systems and software, our methodology will only analyze NDVI data in contiguous clusters large enough to be representative of a complete plant approximately 0.5m^2 (200 pixels) in size. Using ArcGIS's Reclassify, Region Group, and Raster to Polygon tools, we generated a mask that would exclude any NDVI values outside the appropriate size and grouping thresholds. (See **Appendix 3** for the ArcGIS ModelBuilder workflow.)

Once the masked NDVI layer was generated, raster values were normalized so that values range from -1 to 1 using the following raster calculation formula:

$$Normalized\ Value = (Input\ NDVI/127.5) - 1$$

Once normalized, NIR signatures were calculated from a reconfiguration of the original NDVI formula:

$$NDVI = \frac{(NIR - Red)}{(NIR + Red)}$$

$$NIR = \frac{(Red) * (1 + NDVI)}{(1 - NDVI)}$$

The NIR band was stacked with the RGB imagery to create a 4-band raster image, which serves as the input data of the supervised classification procedure.

NDVI Layer to NIR for Classification Input

NDVI alone can help identify areas with photosynthetically active (or live) vegetation, but NIR data can help distinguish plant species that differ in their reflectance. Using the recovered NIR data, unique spectral signatures of the various plant species can be used as training input data for our classification. (See **Appendix 4** for the ArcGIS ModelBuilder workflow.)

Generation of Invasive Plant Training Data for Supervised Classification

To perform supervised classifications in ArcGIS, confirmed presence training data must be generated in order to discriminate distinct plant classes with respect to spectral and textural uniqueness. Using the Classification toolbar in ArcGIS, we drew training polygons over confirmed plant targets whose georeferenced locations were identified during ground truthing trips or via visual comparison to confirmed ground truthed examples. We drew the training samples conservatively, staying well within the spatial extent of each plant to reduce false positives in our classification results. The plants we selected for classification were tamarisk, shortpod mustard, tree of heaven, and tree tobacco. (See **Appendix 5** for photos and descriptions of the plants chosen for training data.)

Supervised Classification

Once the NIR data was recovered from the red and NDVI data, it was composited with the 3-band RGB imagery data to make a 4-band image (NIR+RGB). Using the ArcGIS Maximum Likelihood Classification tool, four defined classes of plants were differentiated from training samples (Table 1). Reject fractions were conservatively set to 0.25, meaning cells were only classified to one of the four defined groups if there was at least a 25% level of confidence. This was purposefully set to favor overclassification of vegetation over omitting detection of potential weeds.

Table 1. *The number of presence sample used to train the classification model to identify and discriminate between different invasive weed species.*

Species	***# of Positive Samples (Present)***
Tamarisk	10
Shortpod Mustard	10
Tree of Heaven	3
Oaks	3

Classification: Object-based Discriminant Analysis

Image Pre-Processing

Image pre-processing consisted of using GDAL to reproject the two sets of drone imagery into NAD-83 UTM zone 11N (the Conservancy's preferred projection), and clipping them to the same spatial extent. The spatial subset was chosen so all imagery overlapped within the region and all ground truth data fell within the boundary. Single-band rasters were extracted from the RoboHawk Phantom 4 three-band imagery. We resampled NDVI imagery from the AeroVironment Quantix drone to match the spatial resolution of the RoboHawk Phantom 4 imagery. We created a fifth grey-level raster comprised of an adjusted difference between the green and red bands of the RoboHawk Phantom 4 imagery. The green-red difference was adjusted so all values were positive, as required by the texture algorithm. This fifth grey-level raster was included since valuable information about vegetation is present not only in the relative magnitudes of red and green reflectance values, but also in the differential between them. These five single-band rasters were input to the texture feature calculations (**Figure 6**).

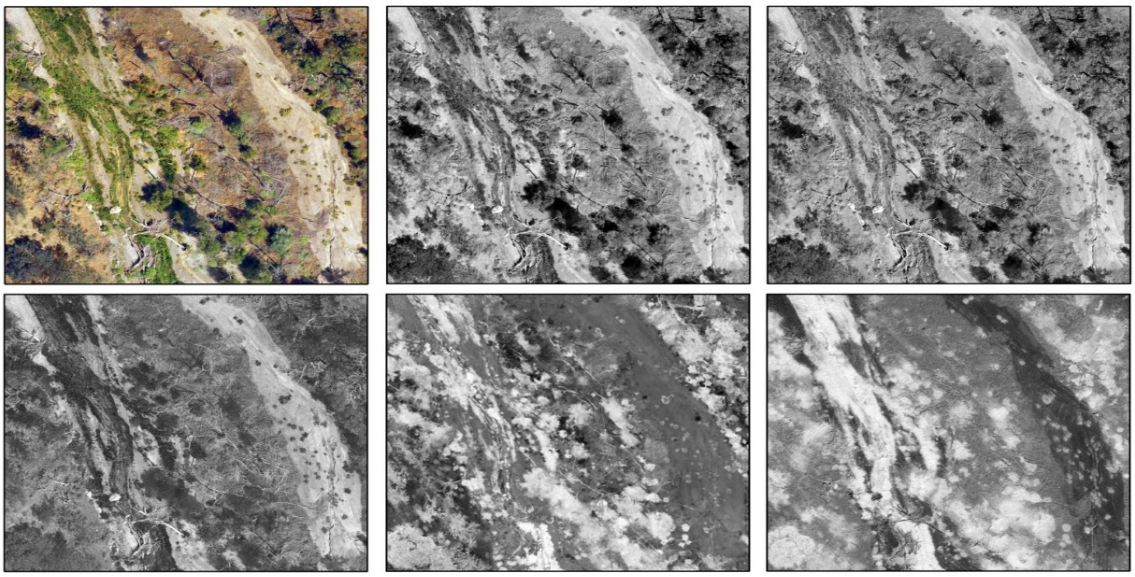

Figure 6. *Zoom of five input raster layers for texture feature derivations. Top row from left to right: original image, red, green. Bottom row from left to right: blue, green minus red, NDVI.*

Segmentation for Object Based Analysis

A segmented polygon layer described regions over which to calculate grey-level texture features within the drone imagery. We created this layer using ArcGIS's Segment Mean Shift tool, which generates a raster with pixels grouped by with adjacent pixels with similar spectral characteristics, creating "segments" of relative spectral homogeneity. We converted these

regions to a polygon feature layer with unique polygon identification numbers, as the texture feature calculation requires a polygon input to outline regions of the grey-level raster over which to calculate texture features. The Mean Shift tool has four parameters: a minimum number of pixels to be included in a segmented region, the bands to use in determining the segmentation, and spatial and spectral detail parameters. The minimum number of pixels was chosen to be 8000 (approximately nine square feet.) The model was run with many different combinations of spectral and spatial detail, with the best combinations identified by inspection. Spectral detail was set to 17 and spatial detail to 16 to obtain the segmented layer that was used in the final analysis. These two parameters indicate the level of importance given to spectral differences and proximity between features in the imagery, respectively. Smaller values result in more smoothing while larger values result in more detail.

Texture Feature Calculation

Grey level co-occurrence matrices record how often specific pixel values occur adjacent to each other. Texture features are statistical quantifications of spatial patterns of raw pixel values and the grey-level co-occurrence matrices. We calculated twenty-five texture features for each of the five grey-level bands discussed in the previous section (**Appendix 6**). These features are the same as those in the R "radiomics" package, and were calculated in ArcGIS via the R-ArcGIS Bridge (**Appendix 7**). We joined the resulting texture feature values to the original segment polygons in ArcGIS to allow visual evaluation of the results (see **Appendix 8** for R scripts and **Appendix 9** for complete texture analysis workflow).

Discriminant Analysis for Tree of Heaven & Tamarisk

We conducted a discriminant analysis based on Gaussian finite mixture modeling using the MclustDA function of the "mclust" package in R. Discriminant analysis tests whether certain combinations of features can resolve species into distinct groups, or differentiate them sufficiently to create a probability-based classification. We selected this method because ground truth data inputs are a set of discrete, known groups. The R package was used so that z-scores, which indicate level of certainty for a given prediction, could be visualized.

We tested multiple combinations of texture features in multiple discriminant analysis model runs, selected based on visual inspection, suggestions from the literature, and physical principles vegetation structure and light reflectance. The clustvarsel function from the R package "clustvarsel" was also used to find different possible combinations of features to test. The clustvarsel functions aid in identifying locally optimal subsets of variables with group/cluster information. The discriminant analysis scatter plots were inspected and

estimated models were run on the entire segmented polygon dataset to assess the predictive capacities of the methodology.

3.3 MaxEnt

MaxEnt, a species distribution model, was used to determine potential areas of invasive plant species occurrence at Tejon Ranch. We chose MaxEnt because it has been shown to perform more accurately compared to other predictive models (Hoffman et al., 2008). MaxEnt uses presence data and environmental variables to predict species occurrence across a landscape. Presence data for plant species was sourced from the 2016 Incidental Weed Encounter Data provided by the Conservancy staff. These data points were collected incidentally as the Conservancy staff encountered invasive plant species while performing various other monitoring tasks, and are therefore not a comprehensive data set. Because we were limited by data (most species consisted of around 30 data points), we focused our modeling efforts on tamarisk because it had the largest data set (297 locations).

We used tamarisk presence data in conjunction with nine environmental layers in MaxEnt version 3.3.3. These layers included slope, aspect, distance from major streams, distance from utilities, distance from cattle corrals, climate water deficit, maximum temperature, precipitation, and soil classification, all with a spatial resolution of 30 m. Slope and aspect were derived from a 26 m digital elevation model using ArcGIS's Slope and Aspect tools. The Euclidean Distance tool was used to calculate the distance from corrals, distance from major streams and distance from utilities. Major streams (classified as having water year-round), corrals, and the utility layer were provided by the Conservancy. Climate water deficit, maximum temperature, and precipitation were acquired from the California Basin Characterization Model (CA-BCM 2014), which uses monthly averages from 7CMIP-3 GCM+SRES models from 1981-2010 to compute averages at 270 m resolution (2014 California BCM). The soil classification layer was acquired from State Soil Geographic (STATSGO2) and was classified by soil order: alfisols, andisols, aridisols, entisols, histosols, inceptisols, mollisols, ultisols, and vertisols. A minimum convex polygon was created around the tamarisk presence data using the minimum bounding geometry tool in ArcGIS and was used as the bias file.

MaxEnt was run using the following parameters: 5000 maximum iterations, 0.00001 convergence threshold, 0 adjust sample radius, 25 random test percentage, 1 regularization multiplier, 10000 maximum number of background points, 15 replicates, and subsample replicated type.

3.4 Cost Benefit Analysis

Deploying drone technologies can be expensive; thus, we deemed it prudent to conduct a cost-benefit analysis (CBA) on two monitoring options that incorporate drones as a means of improving the effectiveness of tamarisk management (Table 2).

Table 2. *A description of the two drone integration options evaluated for the Conservancy.*

Option 1	Purchasing a drone and completing all flights, maintenance, and image acquisition in-house
Option 2	Contracting a drone service to complete flights and all related image acquisition activities

Option 1 consists of purchasing a commercially available drone, a variety of associated accessories, an NIR sensor unit, undergoing the necessary training and permitting, and subscribing to an image pre-processing (stitching and geolocating) service. Option 2 consists of contracting a drone consulting firm to conduct flights and deliver pre-processed imagery to the Conservancy. This analysis is limited to only the acquisition and image stitching process, and excludes any classification endeavors that the Conservancy may choose to pursue. The metric used in this analysis was the Benefit-Cost Ratio (BCR), interpreted as shown in Table 3 below.

Table 3. *Explanation of benefit-cost ratio (BCR).*

BCR Value	***Interpretation***
1	The baseline of status quo weed monitoring activities conducted by the Conservancy
> 1	Indicates that the activity is more beneficial than the status quo
< 1	Indicates that the activity is more costly than the status quo

Costs and benefits for this analysis were accrued over a five-year period. This relatively short period was chosen due to the rapidly improving nature of drone and sensor manufacturing technology. We assume that cheaper, more efficient drone models will be available for commercial use within the next decade, so the time frame in which this CBA is relevant is inherently limited. We completed the CBA under the critical assumption that plant identification after image acquisition is as accurate as status quo monitoring activities.

Costs

The costs associated with Option 1 include the purchase of a commercial drone and accessories, NIR sensor, subscription to an image stitching software service, FAA drone pilot certification and drone registration, and an insurance/ repair policy package from the drone manufacturer (See **Appendix 10** for an itemized list of costs).

In order to estimate the cost of contracting a drone service for Option 2, we asked RoboHawk Aerial Video & Imaging to provide us with a quote for the flight that they completed for us over Panofsky Field. Using this information, we extrapolated from the hourly rate quote we received from RoboHawk to estimate the annual cost of contracting a drone service to replace current weed monitoring activities, with drone flights occurring once a month. RoboHawk estimated 10 hours for one full flight session over an area the size of Panofsky field, end-to-end including image processing. We assume that after purchasing the equipment in Option 1, Conservancy staff would operate on this same 10-hour per month flight schedule.

Benefits

Benefits for both options were calculated in terms of time savings. We calculated the benefits of both options by comparing the decrease in staff man-hours in the field that is afforded due to drone implementation. Specifically, the reduction in hours from field surveying a site the size of Panofsky once per month, down to a 10-hour flight session (once per month). Benefits were made comparable between the two options by using survey information from Conservancy staff about the amount of time it would normally take to complete a systematic survey of Panofsky field on foot. Benefits were discounted at a rate of 7%, which is the convention for most non-profit financial analyses (Ligane 2004).

4. Results

4.1 Flights

RoboHawk and AeroVironment Flight and Mosaic Results

Both drone platforms rapidly collected still images for generating orthomosaics. The Phantom 4 used in the RoboHawk flight produced high quality maps in the DroneDeploy app at 5 cm/pixel (at 200' AGL) and 1 cm/pixel (at 120' AGL). The Phantom 4 captured imagery at the highest resolution of 1 cm/pixel because its hover capabilities reduce motion blur and allow for stable image capture. The Quantix captured imagery at 2.5 cm/pixel (at 360' AGL). True color output maps were created for both Phantom 4 (**Figure 7**) and Quantix flights (**Figure 8**).

Of the image mosaicking solutions, we found DroneDeploy to be the better option due to the quality of the stitched mosaics (lack of blur, smearing, or loss of data). Image mosaicking with AeroVironment's Decision Support System (DSS) yielded mostly positive results. It was able to perform a quick stitch in the field and also cloud-based generation of the final mosaic map. AV's DSS had difficulty cleanly stitching senesced plants, which lack the significant leaf canopy structure that provides a proper stitching reference. Areas with adjacent or overlapping plants were sometimes observed to have smeared into undefinable vegetative regions.

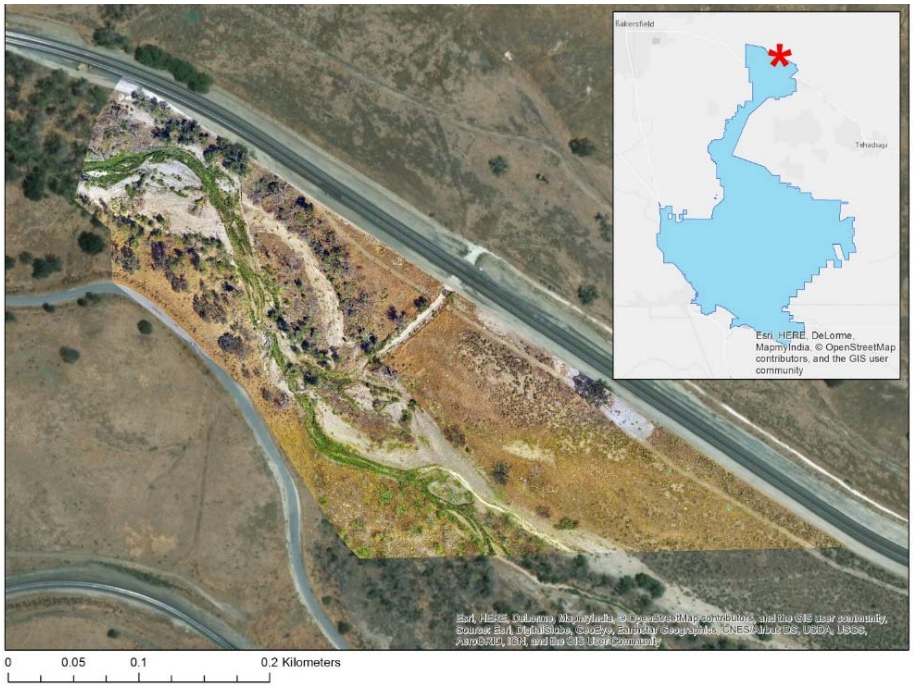

Figure 7. *The mosaicked image of Panofsky Field taken by RoboHawk's DJI Phantom 4 Advanced quadcopter.*

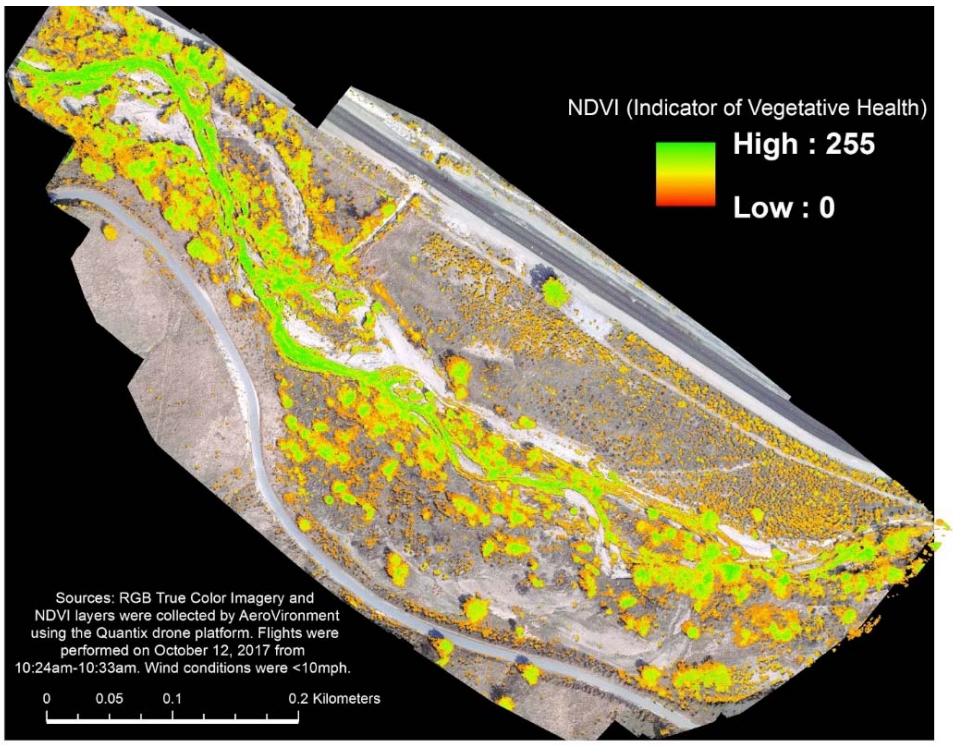

Figure 8. *The mosaicked image of Panofsky Field taken by AeroVironment's Quantix fixed wing.*

4.2 Image Processing

Pixel-Based Maximum Likelihood Classification Results

Ground truthed plant presence data provided reference locations for generating training sample data. At each ground reference location, species were identified and confirmed so that they provide example "search images" for Conservancy staff to match with non-referenced plants in the mosaic imagery. The results from the maximum likelihood classifier tool were displayed as color-coded plant class estimations across Panofsky Field (**Figures 9 & 10**).

The classification yielded mixed results. Tamarisk was overestimated in dry areas near the railroad in the northeastern region of the parcel, where we have confirmed no presence of tamarisk. However, the classification accurately identified isolated individuals in the dried creekbed. Oak trees and cottonwoods were incorrectly classified as tamarisk in densely covered areas in the northwest end of the parcel. There were considerable false positive

assignments to the tree of heaven class, with training data sourced from only from three defined samples. Oaks were more successfully identified throughout the maps, with stand alone oaks were more accurately classified than clustered trees. The classification tool was most successful in identifying shortpod mustard. Most mustards were found northeast of the creek with sufficient spacing to distinguish individual plants.

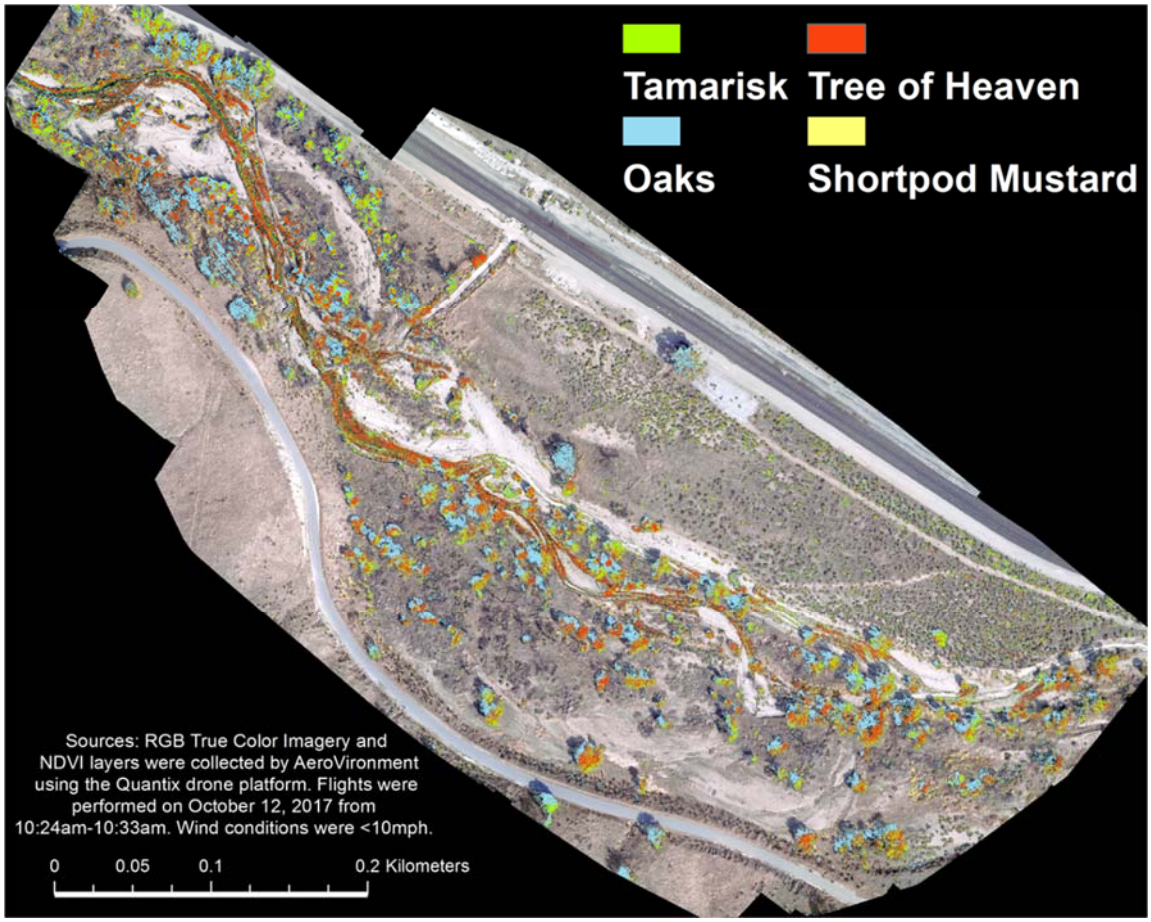

Figure 9. *Results of the pixel-based maximum likelihood image classification. The plants identified by the program are noted in the legend above.*

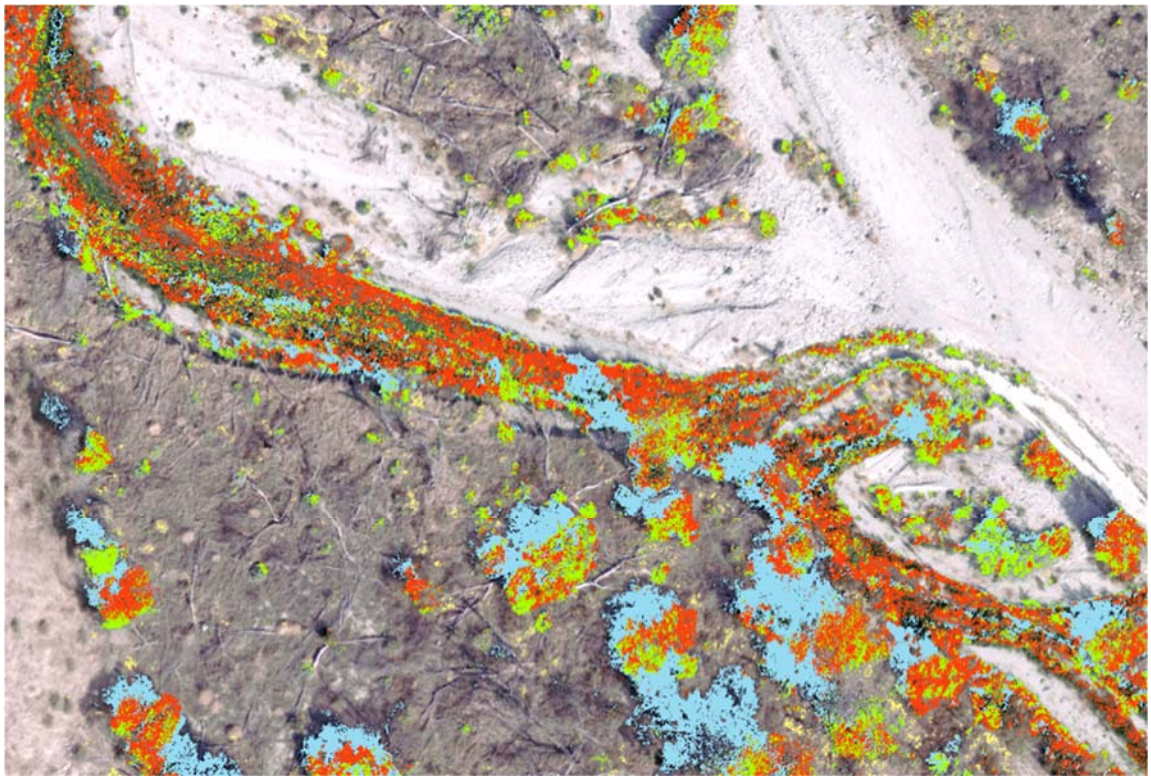

Figure 10. *A closer look at the resulting classifications at Panofsky Field. Tree of Heaven is displayed in red, Shortpod Mustard in yellow, oaks in blue, and Tamarisk in green. This close-up view demonstrates the misclassification that resulted from our analyses, as there appears to be overlap of species identified on the same plant.*

Object-based Discriminant Analysis Classification Results

Segmentation & Texture Features

The final segmentation scale is finer than individual trees but occasionally larger than smaller individual plants (**Figure 11**). It is not especially sensitive to different sizes of plants; the segmentation is more sensitive to homogeneous patches than individual plants, though in some cases these are the same thing. The approximately 20-acre region of interest was segmented into 42,077 polygons.

Figure 11. *LEFT: segmentation layer of the full region of interest in the northeast section of Panofsky Field; RIGHT: A close-up of the segmented polygons layer overlaid on top the DJI Phantom 4 imagery.*

The texture in some cases helps distinguish between different general classes of land cover, but do not clearly distinguish different species of interest from this imagery (**Figure 12**).

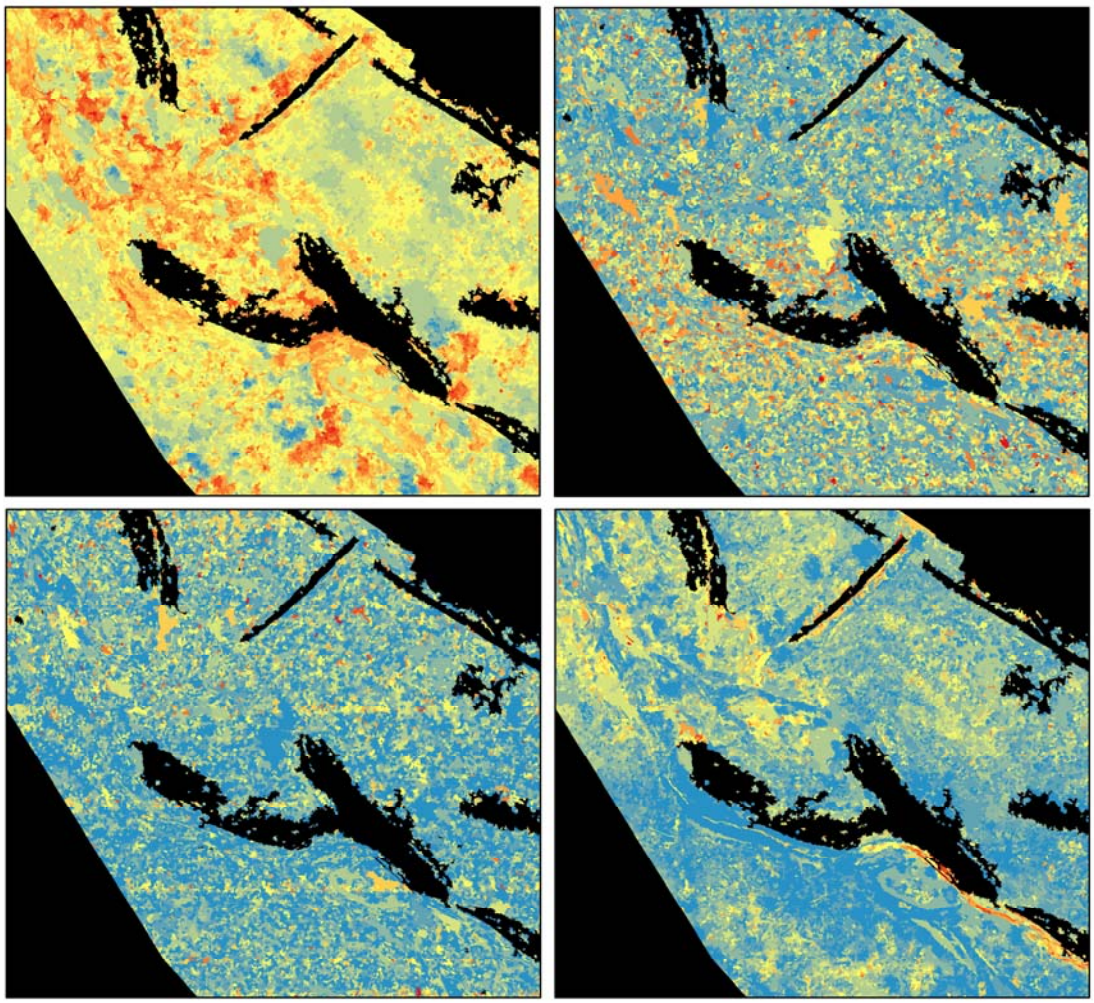

Figure 12. *Four of the texture features used in the classification. Clockwise from top left are: NDVI entropy (first order), band 1 GLCM difference entropy, band 1 GLCM cShade, and band 2 GLCM homogeneity 1. In the second and third images, a residual linear streaking effect from the flight pattern and image stitching is apparent.*

Discriminant Analysis

Discriminant analysis revealed that neither tree of heaven nor tamarisk could be classified algorithmically from texture features using 1cm resolution 4-band imagery taken in mid-September, to a useful degree of accuracy. The discriminant analysis scatterplots show that presence and absence points overlap almost completely, and that calculated centroids are not sufficiently far apart for the species to be accurately classified algorithmically in the imagery. The most accurate classification of tree of heaven had a training error of 0.15 (**Figures 13 & 14**). With 51 true positive and 26 false positives, the model's precision was 66.2% (**Appendix 11**). However, the model had a low percentage of false negatives, as only 9 of 60 presence points were classified by the model as "absence" points.

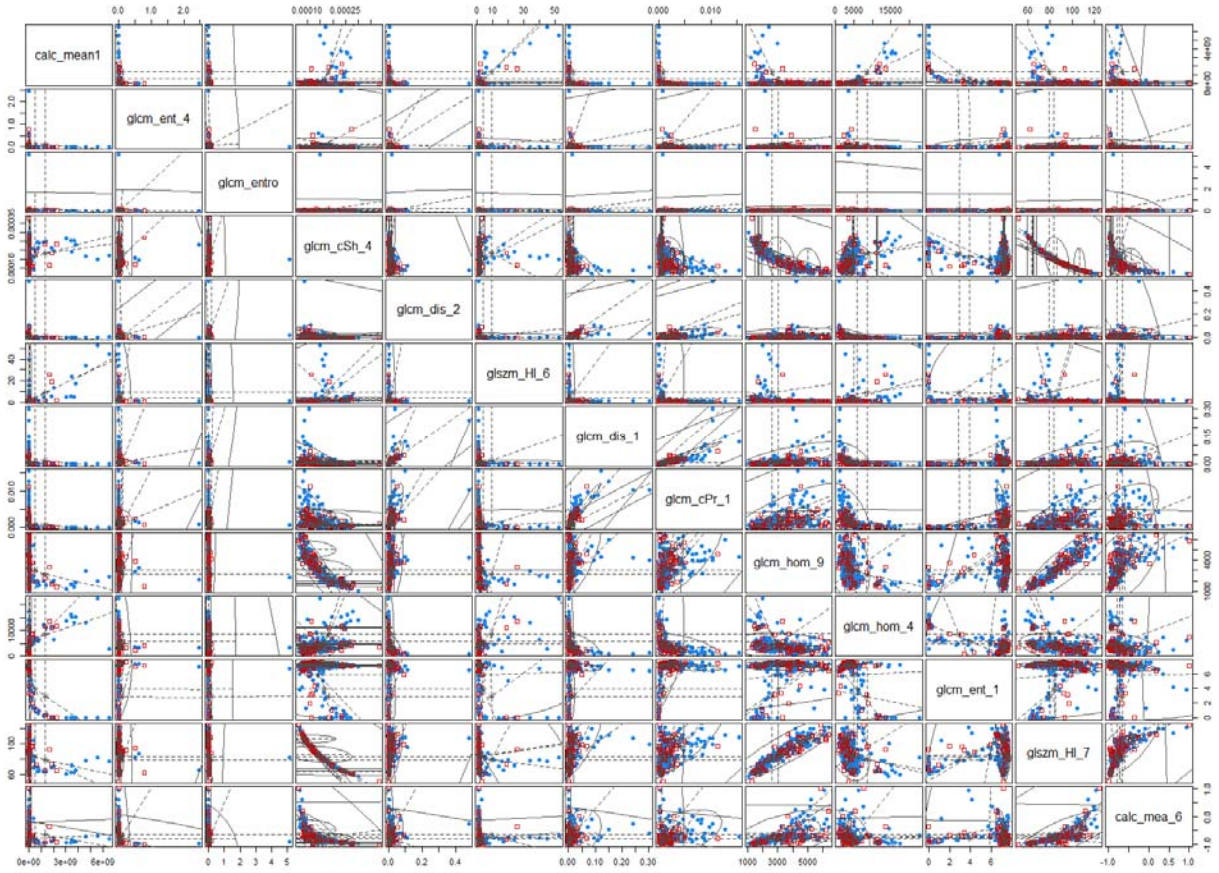

Figure 13. *The discriminant analysis scatterplots generated from one tree of heaven analysis, demonstrating the lack of precision of this type of analysis in this case.*

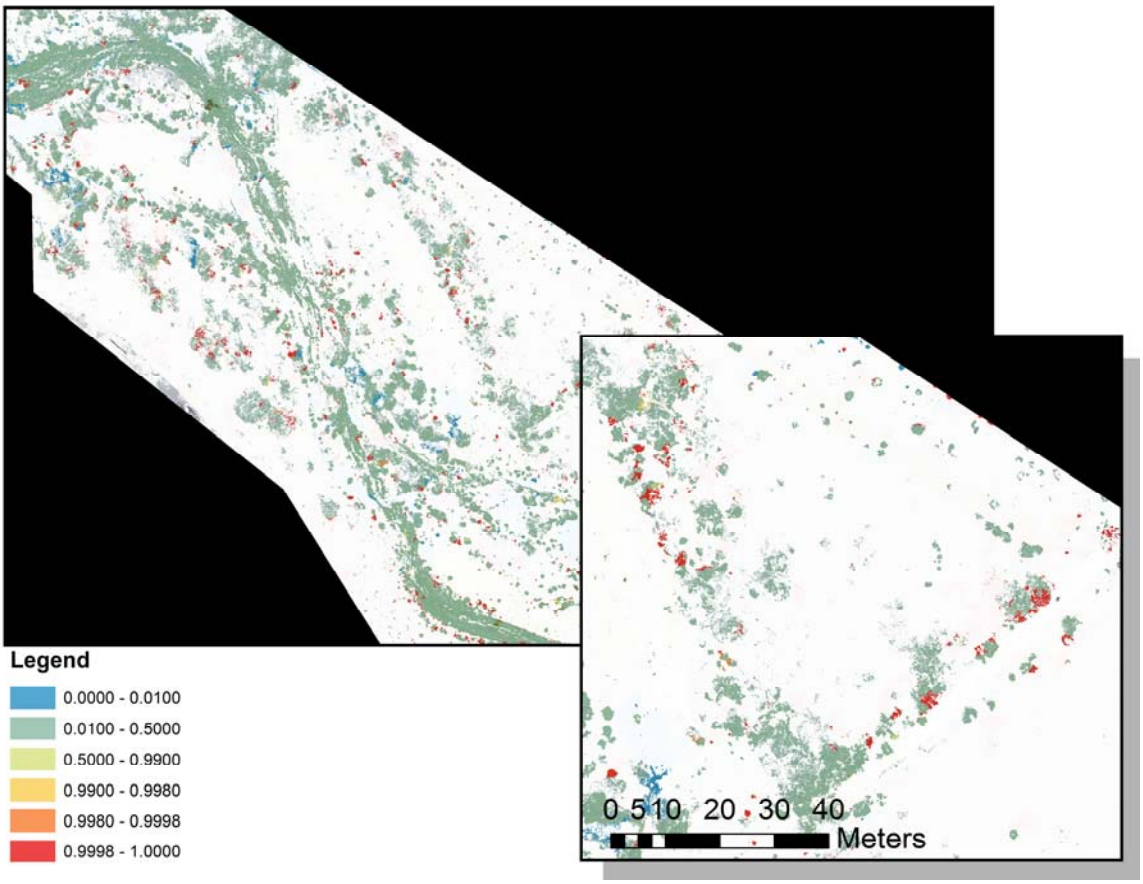

Figure 14. *The map output from the discriminant analysis of tree of heaven. Legend values correspond to confidence in tree of heaven presence, as determined by the discriminant analysis. Analysis was based on 133 confirmed absence and 60 confirmed presence points, and 13 texture features (**Appendix 6**).*

4.3 MaxEnt

Our results show that tamarisk probability of occurrence is highest along major streams (**Figure 15**). Predictions of tamarisk occurrence were fairly accurate with an area under the curve (AUC) of 0.989. Major streams had the largest contribution followed by soil type. All other variables had low (<5%) contribution.

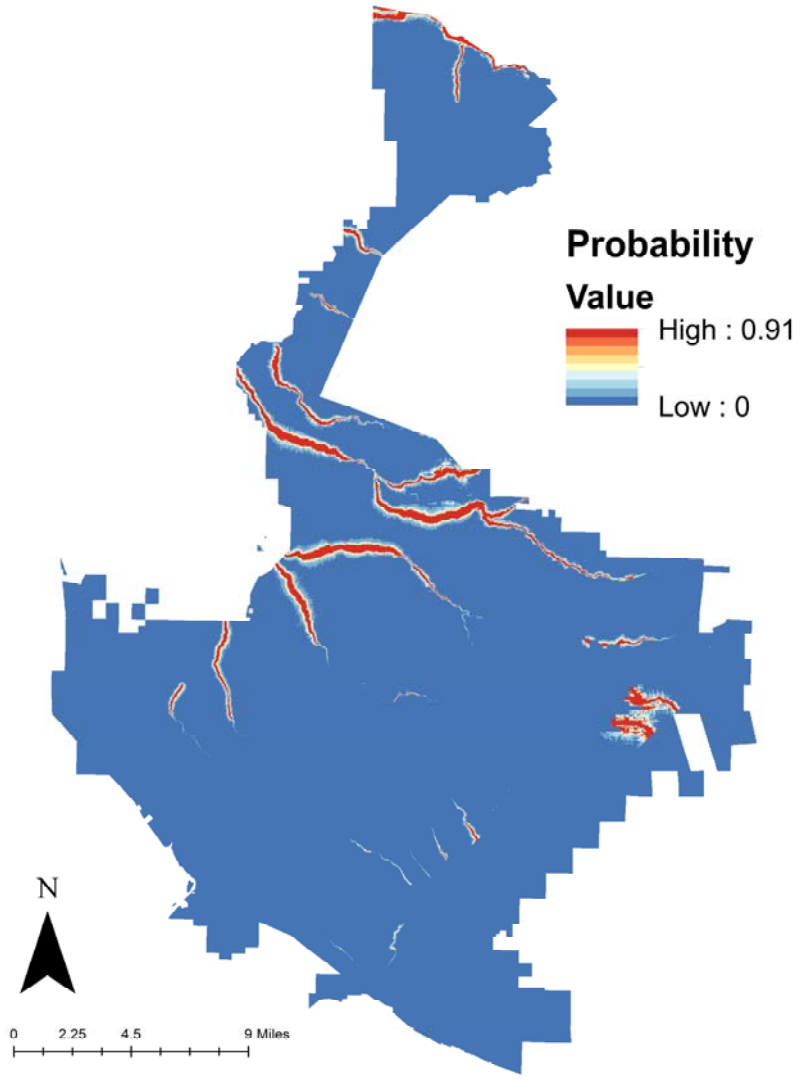

Figure 15. *Probabilistic distribution of tamarisk at the Tejon Ranch Conservancy in California based on 297 presence locations and nine environmental factors. Red colors indicate an area with a high probability of tamarisk distribution and blue colors indicate an area with a low probability of tamarisk distribution.*

4.4 Cost Benefit Analysis

The CBR of Option 1 (drone purchase) was calculated to be 1.15, while the CBR of Option 2 (drone service) was 0.15. Option 1 is clearly to be the more desirable of the two, and would return a net present value of $ 3,797.35 in benefits over the five-year period.

5. Discussion & Conclusion

5.1 Ground Truthing & Flights

Ground Truthing

For future UAVs flights at Tejon Ranch, establishing training areas before flying and collecting imagery can be useful to accurately identify and geographically locate plant species such as invasive weeds and conifers. When selecting training areas, the Conservancy should obtain a representative sample of plant species of interest in a wide variety of phenological stages present in the area during that flight season. The more descriptive information obtained about each training area plant, the more easily and accurately each individual plant can be identified from the aerial imagery.

In this study, training area black arrow signs with rectangular cardboard dimensions of 10" x 18" were sufficiently large enough to locate them in the high resolution (0.4 inch/pixel) Phantom 4 drone imagery flown at 120' AGL. They were almost as well distinguishable in the 200' AGL and 2-inch/pixel resolution imagery of the same drone. In the Quantix drone imagery, flown at 360' AGL with imagery of 1 inch/pixel resolution, these training area signs were more challenging to identify. Therefore, the Conservancy may consider increasing the sign dimensions to approximately 14" x 22" when flying this drone to ensure that all training areas can be sufficiently located and identified in the imagery. Also, the training area signs for the Quantix drone imagery may be more discernable from barren soil by instead using red or yellow arrows with black borders and white cardboard backgrounds. Ultimately, materials and colors used to create these signs should minimize reflectance in the imagery by avoiding use of shiny materials.

A minimum of 30 training areas should be used, or more until representative libraries of the plant species of interest are obtained. For repeat flights over the same field site during different seasons, ground truthing should be repeated to account for differences in phenology of plant species (i.e. dropped leaves, changes in color, senescence, flowering, etc.).

Overall, for future UAV imaging flights at Tejon Ranch, ground truthing prior to flying is extremely useful, and in most cases necessary, to properly identify and locate individual plant species of interest such as invasive tamarisk.

Flights and Image Mosaicking

Details on characteristics associated with drone-specific design can be reviewed in Section 2.4 (UAV Design). Comparing a fixed wing platform (Quantix) against a quadcopter platform (Phantom) for capturing vegetation data, we found that the Phantom can collect data at higher spatial resolutions while the Quantix was able to collect data at higher spectral resolution with its NIR sensor. The Phantom had more flight flexibility in terms of altitude, and angle of image capture (for 3D modeling applications), and hovering to focus on a target of interest. The Quantix has fixed aperture sensors, which require a fixed altitude of 360' AGL. Although we did not test the video capabilities of the Phantom, we are confident that this feature can also be used for qualitative assessments that do not require explicit quantitative spatial analysis. DSS's difficulty in stitching senesced plants, and its smearing of adjacent plant outlines, are most likely due to its method of flight. Fixed wing designs can cover more area per flight relative to a quadcopter, but fixed wings must maintain constant forward motion, which can cause image distortion. This is not a major issue for AeroVironment as the Quantix was not designed to identify plants, but rather to assess the health of known crops.

5.2 Image Processing

Pixel-Based Maximum Likelihood Classification

AeroVironment's Quantix provided sufficient spectral data to generate training samples for the classification. Tamarisk was over-classified in areas with confirmed absence. Additional training samples could potentially help with the differentiation of tamarisk from other plant species. Tree of heaven, tamarisk, and oaks were often classified together. Shortpod mustard was classified with the most success; its desiccated stage showed that attention to phenology in flight planning can help optimize the discrimination of specific target plant species. The quality of spectral data can be optimized if flights are planned for when the target plant species is most distinct from surrounding plants.

Object-based Discriminant Analysis Classification

The results of the discriminant analysis showed that neither tamarisk nor tree of heaven could be algorithmically classified from the imagery to a useful degree of accuracy. However, classification may still be feasible, as shown in other studies, if imagery is collected at carefully chosen times of the year and with sensors capable of much higher spectral resolution. Species-level classification is not feasible without a carefully designed strategy, which requires identifying times when the species is phenologically or physiologically distinct from

surrounding vegetation. New drone sensors with higher spectral resolution could make detection of invasive species feasible and affordable within the next decade, as such technologies already exist and rapid market expansion is generally causing prices of drone technology to decline due to the increased competition and continuous innovation. With additional presence/absence data on species of interest, it should be possible to start disentangling the optically distinct patterns and phenological schedule. To assess the full potential of classification by features analysis, more presence/absence data is needed.

5.3 MaxEnt

Our results show that distance from major streams was the most important variable for predicting tamarisk occurrence at the Conservancy. These results agree with a previous study that modeled tamarisk distributions using MaxEnt in Nebraska (Hoffman et al., 2008). Tamarisk occurrence was also associated with slopes close to zero (i.e., flatter areas). Tamarisk was also highly correlated with soil type; however, the spatial resolution of the soil layer was quite coarse. Higher resolution soil data might improve the accuracy of the model.

To further improve this model, more tamarisk presence locations are needed. Though there are 297 presence locations for tamarisk, most of them are congregated in two main areas. The Conservancy should collect more tamarisk presence locations points to better inform the model.

The MaxEnt output can be used to inform the Conservancy on where to fly drones to monitor for tamarisk. Note that if the Conservancy surveys an area MaxEnt indicated as having a high probability of tamarisk occurrence, but none is discovered, it does not mean the model is wrong, it could simply mean that tamarisk has not dispersed to that region. The only way to inform the model is to increase the amount of presence data. Moving forward, this same model can be used for other invasive plant species of interest at the Conservancy. However, Conservancy staff need presence locations from multiple areas on the Ranch to produce a MaxEnt output with high confidence.

5.4 Cost Benefit Analysis

While there is a significant difference between the BCRs of the two proposed options, the resulting benefits are modest. Option 1's BCR is 1.15, which means that for every $1.00 of cost for the project, there is a $1.15 return, and the net present value of benefits for Option 1 was only $3,797.35 over five years ($19,440.00 before discounting). This may not be enough of a benefit to persuade the Conservancy to move forward with purchasing a drone.

However, our analysis is limited to only the benefits in terms of avoided future costs of tamarisk removal. Were this analysis expanded to include ecological benefits of other monitoring targets of interest to the Conservancy –including other invasive weed species and conifer mortality - the resulting BCR could be significantly higher. In addition, our estimates of potential costs for Option A were intentionally high in order to produce a conservative estimate. This intentional overestimation of costs and underestimation of benefits demonstrates that despite a high first year of invest cost, the benefits of this technology, when more accurately quantified, would only increase.

6. Recommendation

After an extensive literature review regarding the use of drones in conservation research, as well as a demonstration on a threatened landscape, we confirmed that drones, if properly utilized, can be a useful tool to expand monitoring reach. However, Tejon Ranch is simply too large and variable in terrain to monitor in its entirety, multiple times per year/as many times per year as would be necessary for detecting invasion of undesirable plant species. Therefore, the Conservancy must be able to prioritize specific areas to target with drone surveys. Our group recommends that drone flights be performed on threatened habitats discerned by our MaxEnt model, with current environmental input data. In addition to targeting key areas in mitigation efforts, presence data derived from inspection of drone imagery can be included in new iterations of the MaxEnt workflow to more accurately predict future invasive plant dispersal risk (**Figure 16**). As the workflow is cycled with continually updated environmental data and new presence data, the overall monitoring framework becomes more robust and efficient.

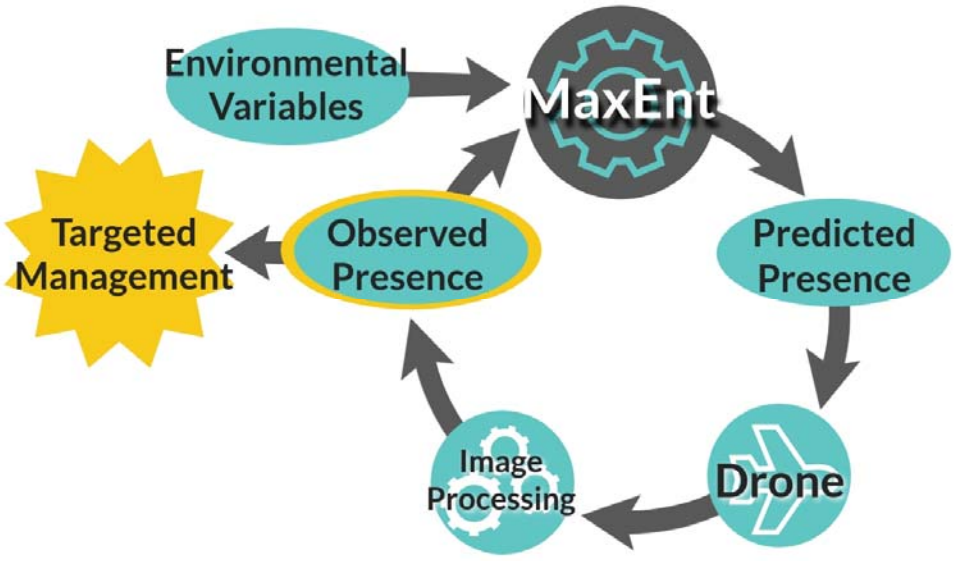

Figure 16. Recommended framework for incorporating drone technology into ecological monitoring at Tejon Ranch.

[This page intentionally left blank]

Appendices

APPENDIX 1. Current UAV systems and specifications.

UAV Platform	Price	Design	Stock Sensor	Other Sensors	Flight Time	Approx Coverage Area	Control Range	Interface	Obstacle Avoidance	Georeferencing	Env. Constraints	Replacement Parts	Community	Software
DJI Phantom 3	$500	Quadcopter	2.7K 12MP	Requires specific adapters, Seqouia	25 min	varies w/ resolution+altitude	1 km	Controller+Smartphone	N	GPS	0-40 ºC	Y	Y	DJIGO Control App, No Image Processing
DJI Phantom 3 Advanced	$799	Quadcopter	2.7K 12MP	Requires specific adapters, Seqouia	23 min	varies w/ resolution+altitude	5 km	Controller+Smartphone	N	GPS/GLONASS	0-40 ºC	Y	Y	DJIGO Control App, No Image Processing
DJI Phantom 3 Pro	$999	Quadcopter	4K 12 MP	Requires specific adapters, Seqouia	23 min	varies w/ resolution+altitude	5 km	Controller+Smartphone	N	GPS/GLONASS	0-40 ºC	Y	Y	DJIGO Control App, No Image Processing
DJI Phantom 4	$1,000	Quadcopter	4K 12.4MP	Requires specific adapters, Seqouia	28 min	varies w/ resolution+altitude	5 km	Controller+Smartphone	Y	GPS/GLONASS	0-40 ºC, wind <10m/s	Y	Y	DJIGO Control App, No Image Processing
DJI Phantom 4 Advanced	$1,199	Quadcopter	4K 20MP	Requires specific adapters, Seqouia	30 min	varies w/ resolution+altitude	7 km	Controller+Smartphone	Y	GPS/GLONASS	0-40 ºC, wind <10m/s	Y	Y	DJIGO Control App, No Image Processing
DJI Phantom 4 Pro	$1,500	Quadcopter	4K 20MP	Requires specific adapters, Seqouia	30 min	varies w/ resolution+altitude	7 km	Controller+Smartphone	Y	GPS/GLONASS	0-40 ºC, wind <10m/s	Y	Y	DJIGO Control App, No Image Processing
DJI Inspire 1 V2.0	$1,999	Quadcopter	4K 12MP	Requires specific adapters, Seqouia	18 min	varies w/ resolution+altitude	5 km	Controller+Smartphone	N	GPS/GLONASS	-10-40 ºC, wind <10m/s	Y	Y	DJIGO Control App, No Image Processing
DJI Inspire 2	$2,999	Quadcopter	4K	Requires specific adapters, Seqouia	27 min	varies w/ resolution+altitude	7 km	Controller+Smartphone	Y	GPS/GLONASS	-20-40 ºC, wind <10m/s	Y	Y	DJIGO Control App, No Image Processing
DJI Mavic	$999	Foldable Quadcopter	4K	Requires specific adapters, Seqouia	27 min	varies w/ resolution+altitude	7 km	Controller+Smartphone	Y	GPS/GLONASS	0-40 ºC	Y	Y	
Sensefly eBee	$10,000	Fixed-Wing	Parrot Sequoia	Requires specific adapters	55 min	500acres at 120m AGL, 7400 at 2000m	3 km	Laptop	N	GPS	wind <12/m/s	Y	Y	eMotion Flight software, Pix4d optional
Parrot Disco Pro Ag	$4,499	Fixed-Wing	Parrot Sequoia	Angled forward facing RGB sensor	30 min	200acres at 120m	2 km	Controller+Smartphone	N	GPS/GLONASS		Y	N	AIRINOV (powered by Pix4D)
Lehmann Aviation LA500-AG	$7,990	Fixed-Wing	Parrot Sequoia	Requires specific adapters	35 min	2400acres at 1000m AGL		Laptop	N	GPS	wind <10m/s	Y	N	OperationCenter v2, AgiSoft and Pix4D optional
AeroVironment Quantix	$16,500	Fixed-Wing + 2 rotors	RGB, Multispectral	No	45 min	400acres		Tablet	N	GPS		N	N	Quantix and AV Decisions Support System (AV DSS)
Birdseye Firefly6 Pro	$5,999	Fixed-Wing + 6 rotors	Variable, Thermal, Sequoia	Requires specific adapters, Thermal	45 min	500acres	5 km	Controller+Laptop	N	GPS		Y	N	Produces imagery that can be fed into any post-processing solution
Event 38 E384	$2599 + sensors	Fixed-Wing	Variable, Thermal, Sequoia	Requires specific adapters, Sequoia, RedEdge, Thermal	90 min	1000acres	5 km	Controller+Laptop	N	GPS	wind <10m/s	Y	N	Pixhawk flight controller, optional post-processing software
O'qualia Captor	$5,990	Fixed-Wing	Sony WX500	Requires specific adapters, Sequoia, Sony RX100	50 min	3500acres at 152m AGL		Tablet	N	GPS	wind <12.5m/s	Y	N	UgCS Mission Planning software

Sensors	Parrot Seqouia	Canon S110 NIR / Red Edge	FLIR Duo / Duo R	FLIR Vue	Micasense Rededge	Sentera Double 4K Ag	Sentera Single NDVI & NDRE
Costs	$3,500	$600-$1000	$999/$1299	$1499-$3199	$5,195	$2499-$4299	$1999-$2799
Sensor Type	RGB, Multispectral	Converted NIR/RE	Thermal + HD visible	Thermal	RGB, Multispectral	4K HD RGB, Multispectral	Multispectral
Advertised Resolution	16MP RGB, 4x 1.2MP bands	12MP	Thermal (160x120), 2MP color, 1080p liveview	(336x256) or (640x512)	3.6MP RGB	12.3MP Stills, 4K Vid @ 30fps	1.2MP stills, 720p video
Spectral Band	4 bands: G,R, RedEdge, NIR	NIR/ RE	7.5-13.5microns (IR Thermal)	7.5-13.5microns (IR Thermal)	5 bands: B,G,R,RE,NIR	5 bands: B,G,R,RE,NIR	5 bands: B,G,R,RE,NIR
Compatible UAVs	DJI, Parrot Disco, Sensefly eBee	Sensefly eBee, Event38, more	DJI, adapters available, similar to GoPro dimensions	DJI Inspire/M100 (larger sensor)	DJI, Sensefly eBee	DJI,Sentera Omni, Sentera Phoenix	DJI, Sentera Omni, Sentera Phoenix
Design Intention	Ag/Research	Converted Point + Shoot	Thermal Inspection/ Search + Rescue	Thermal Inspection / Search+Rescue	Ag/Research	Ag/Research	Ag/Research
Weight	135g	172g	84g	101-122g	175g	80g	30g
Notes	Includes sunshine sensor and cable	Converted to NIR, standard camera pre-conversion is ~$500	R has radiometric temp measurements, shaped similar to GoPro, resolution may be too coarse for ranged monitoring	Gimbal sold seperately	Includes sunshine sensor and cable	Voids DJI warranty, incident light sensor sold seperately ($549)	Voids DJI warranty, incident light sensor sold seperately ($549)

Software	Cost/Format	Subscription	Perpetual License	Operational Range	Compatible UAVS	Compatible Sensors	Notes
SenseFly eMotion 2 & 3	Included with eBee drone	N	N	3km	SenseFly eBee, rotor UAVs	Seqouia, Point and Shoot Cams, eBee compatible	Can export to Pix4D
MicaSense ATLAS Flight	Free iOS App	N	N	Variable with platform	DJI only	DJI cams, RedEdge, Seqouia	Ability to plan battery change sites during missions
AV Decision Support System	$3000/year	Y	N		AeroVironment Quantix	AeroVironment Quantix built-in sensors	AeroVironment's proprietary software, comes with tablet controller
DroneDeploy	Free iOS/Android App, Pay for Premium Features	Y	N	Variable with platform	DJI only	DJI Cam	Streamlined upload to output 3D models/orthomosaics with Pix4D
Pixhawk (Open Source)	$150-$200 for controller, Open Source	N	N	Variable with platform	Open-Source, Home-built	Seqouia, Point and Shoot Cams	Open source so it will not be "ready to fly" immediately out of box
Pix4D Mapper Pro	$8700 standard pricing	Y	N	Variable with platform	SenseFly eBee, rotor UAVs (DJI, 3DR)	RedEdge, Seqouia, HD RGB	$4990 Non-commercial license, $350/mo or $3500/yr standard pricing
Maps Made Easy Map Pilot	$10 iOS App (iOS v8+)	N	Y	Variable with platform	DJI only	DJI Cam	Calculates battery changes, optimized to create georeferenced orthophotos, 3D models, DSMs, NDVI, etc with the pay as you go map processing fees

Software	Cost	Subscribe Option	Operating System	Controller Interface	Features / Services	Output	Additional Notes
Pix4D	$4,990	Y	Windows 64-bit, iOS, Linux Enterprise	Y	Georeferening with ground control points, photogrametry to generate DSM, measure volumes based on the DSM, project splitting for efficient processing, automatic aerial triangulation to mosaic with or without camera orientation information, automatic color and brightness correction , more	GeoTIFF	Perpetual license is $4990. Private subscription option is $350 per month. Seqouia integration optimized, it has become an industry standard (along with drone deploy)
Maps Made Easy	Varies	N	iOS app, Windows or Mac	Y	3D Model stitching, Georeferencing, Volume Measurement (mining), Map Pilot (iOS), NDVI, cloud processing, multi-map management for time-lapses	GeoTIFF, Textured 3D Model, JPG, DEM, Pt Cloud, KMZ	Pay as you go credit system. May be very cost-effective for conservancy, since it has variable cost according to resolution and area requiring processing
Agisoft Photoscan Standard	$179	N	Mac, Windows, Linux	N	Photogrammetry, Point Cloud Generation, 3D model generation and texturing, Panorama stitching,	JPEG, TIFF, GeoTIFF, PNG, BMP, PPM, KML, PDF, OpenEXR and JPEG Multi-Picture Format (MPO), point cloud formats (Wavefront OBJ, Stanford PLY, XYZ text file format, ASPRS LAS)	Photoscan is industry standard, can calculate area and volume (good for % land coverage and biomass estimates), computationally extensive if generating 3D models
AgiSoft Professional	$3,499	N	Mac, Windows, Linux	N	In addition to standard edition: Point Cloud classification, DEM, DSM, DTM, Georeference Orth, Mutltispec, Python script for automized workflows, ground control points, volume measurement, network processing	JPEG, TIFF, GeoTIFF, PNG, BMP, PPM, KML, PDF, OpenEXR and JPEG Multi-Picture Format (MPO), point cloud formats (Wavefront OBJ, Stanford PLY, XYZ text file format, ASPRS LAS)	Photoscan is industry standard, computationally extensive if generating 3D models
AgVault Mobile Edition	$5 / month	Y	iOS only	Y	NDVI, Mobile Mosaicking	shp, data not readily sharable or exportable	Infield quicktiling and NDVI, Highly directed at AG market, Advertizes that it processes files ready for Pix4D, suggesting that this is an intermediadary software, may not be needed if ArcGIS/R is avail to TRC.
AgVault Pro Edition	$29 / month	Y	iOS only	Y	NDVI, Mobile Mosaicking	shp, sharable data requires $12/mo "Viewer's license"	Infield quicktiling and NDVI, Highly directed at AG market, Advertizes that it processes files ready for Pix4D, suggesting that this is an intermediadary software, may not be needed if ArcGIS/R is avail to TRC.
Drone2Map by ESRI	$3500 / year	Y	Windows 7, 8, 10 64 bit	N	2D orthomosaics, 3D Mapping, NDVI, DSM, Cloud Processing, ground control points in field from visual reference points	basemaps, gdb, kml, shp, OBJ, pdf	ESRI's attempt to streamline the process of UAV imagery to final outputs, engine based off of Pix4D, beta testing of integration with DroneDeploy
MicaSense ATLAS Standard	$49 / month	Y	Mac iOS, Windows	Y	NDVI, NDRE, OSAVI, RGB, CIR	Multiband GeoTIFF, DSM (reqrs Pix4DPro)	Powered by Pix4D, Dataset outputs user friendly to switch between spectral bands/indices, Not a start to finish software
MicaSense ATLAS Premium	$99 / month	Y	Mac iOS, Windows	Y	NDVI, NDRE, OSAVI, RGB, CIR, Chlorophyll	Multiband GeoTIFF, DSM (reqrs Pix4DPro)	Powered by Pix4D, Dataset outputs user friendly to switch between spectral bands/indices, Not a start to finish software
DroneDeploy	$83-249 / month	Y	Mac iOS, Windows	Y	NDVI, Elevation, Georeferencing	JPEG, GeoTIFF, shp, Countours, Point Clouds	Used for trial flights at Panofsky, Higher end users get processing priority in queue

APPENDIX 2. Publically accessible databases that house spectral and spatial data, and remote sensing resources.

Resource	URL
Earth Explorer USGS Spatial Data Portal	https://earthexplorer.usgs.gov/
USGS Landsat Data Viewer	https://landsatlook.usgs.gov/viewer.html
Planet Explorer Beta	https://www.planet.com/products/explorer/
Copernicus Open Access Hub for Sentinel Products	https://scihub.copernicus.eu/
USDA GeoSpatial Data Gateway	https://gdg.sc.egov.usda.gov/GDGOrder.aspx
AVIRIS Data Portal	https://aviris.jpl.nasa.gov/alt_locator/
AVIRIS-NG Data Portal	https://avirisng.jpl.nasa.gov/alt_locator/
NASA LAADS Distributed Active Archive Center (DAAC)	https://ladsweb.modaps.eosdis.nasa.gov/search/
ESA Data Access	https://earth.esa.int/web/guest/data-access/how-to-access-esa-data
EarthData EOSDIS Remote Sensors Table	https://earthdata.nasa.gov/user-resources/remote-sensors
EOPortal Directory: Satellite Missions Database	https://directory.eoportal.org/web/eoportal/satellite-missions
NOAA **Comprehensive Large Array-Data Stewardship System**	https://www.ncdc.noaa.gov/airs-web/search

APPENDIX 3. NDVI cell grouping layer: ArcGIS ModelBuilder workflow.

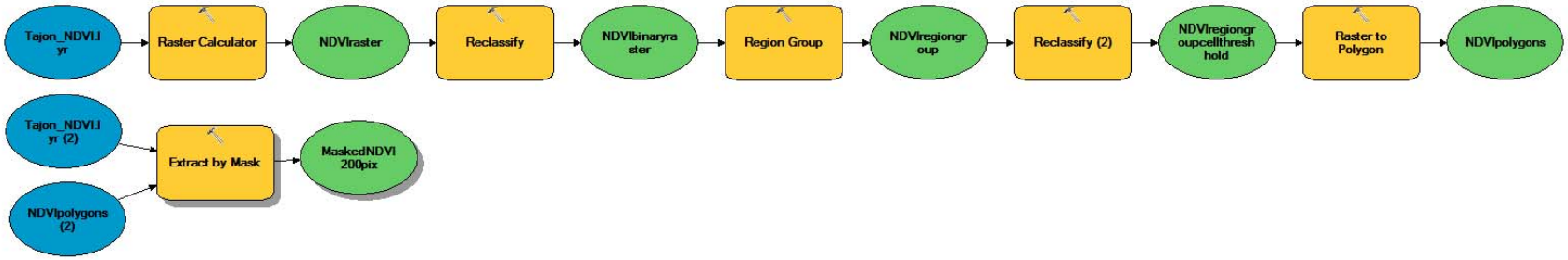

APPENDIX 4. NDVI layer to NIR: ArcGIS ModelBuilder workflow.

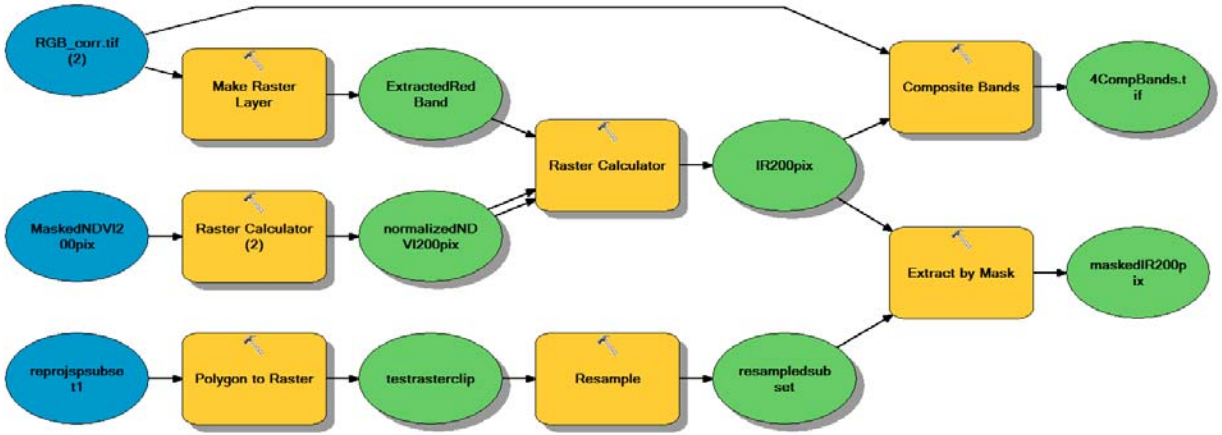

APPENDIX 5. Images and descriptions of the plants chosen for classification training data.

Tamarisk

Tamarisk is a deciduous shrub that maintains gray to jade-colored branches with feathery-scaled leaves. The leaves are highly reduced and thus individual leaves are not visible from aerial imagery. Their thin branches contribute to their irregular top-down shapes. They are primarily near streams due to their intense water demands. In our specific test plot, we mostly observed small patches (1-3 individual plants) in addition to several stretches of young tamarisk running along the creek bed.

LEFT: aerial view of a tamarisk plant; RIGHT: ground view of the same plant pictured in the left panel.

Shortpod Mustard

At the time of the RoboHawk flight (September 2017), most shortpod mustard plants on the parcel were desiccated and dead. Typical plants were yellowish-golden shrubs in color and uniform in their circular shape from an aerial perspective. At this particular phonological stage, they are quite distinct from surrounding living vegetation. Additionally, mustard plants were rarely overlapping in distribution allowing for individual plants to be discriminated more easily with their thin branching structure and singular round shape. There was a large abundance of shortpod individuals on the eastern edge of the parcel near the train tracks, which can be a possible vector. It is especially important to note the differences in phenology because live mustard plants will have active chlorophyll and appear green with small yellow flowers while still maintaining similar aerial silhouettes.

LEFT: aerial view of a shortpod mustard plant; RIGHT: ground view of the same plant pictured in the left panel.

Tree of Heaven

Of our four sample invasive plants, tree of heaven was the largest sized species with distinct opposite pinnate leaf pattern. Individual leaves are visible and are lanceolate shape. Fruiting trees can be more easily distinguished as terminal ends of branches are populated with dense bunches of red seed pods. At the time of the RoboHawk flight (September 2017), few other plants displayed significant clusters of red flowers or seeds, making tree of heaven easy to identify and create training data samples from.

LEFT: aerial view of a tree of heaven plant; RIGHT: ground view of the same plant pictured in the left panel.

Tree Tobacco

Despite having the largest leaf size of our 4 test species, tree tobacco generally has the smallest basal area. At the time of the RoboHawk flight (September 2017), it is observed to be silvery-blue green in color with clusters of yellow tubular flowers. Similar to tamarisk, tree tobacco is observed to be near water sources, as they prefer moist soils. Despite star thistles and sunflowers also having yellow flowers, the blue-silver tint and large leaf area help distinguish tree tobacco.

LEFT: aerial view of a tree tobacco plant; RIGHT: ground view of the same plant pictured in the left panel.

APPENDIX 6. Twenty-five texture features calculated for each of the five grey-level bands, with those used in trial classification of tree of heaven indicated with checkmark.

Features Calculated	Red Band	Green Band	Blue Band	Green-Red Adjusted Difference	NDVI
calc_skewness					
calc_mean	✓			✓	
calc_sd					
calc_entropy	✓			✓	✓
calc_kurtosis					
calc_min					
calc_meanDeviation					
glcm_mean					
glcm_entropy					
glcm_sumEntropy					
glcm_differenceEntropy					
glcm_cProminence	✓				
glcm_cShade				✓	
glcm_homogeneity1		✓			
glcm_homogeneity2				✓	
glcm_dissimilarity	✓	✓			
glrlm_LRLGLE					
glrlm_LRHGLE					
glrlm_GLN					
glrlm_SRHGLE					
glrlm_LGLRE					
glszm_HILAE				✓	
glszm_HISAE			✓		
glszm_LILAE					

APPENDIX 7. Details on the R "radiomics" package and R-ArcGIS bridge.

Documentation on Radiomics R Package

- http://journals.plos.org/plosone/article?id=10.1371/journal.pone.0102107
- https://doi.org/10.1371/journal.pone.0102107.s001
- https://www.rdocumentation.org/packages/radiomics/versions/0.1.1
- http://joelcarlson.github.io/2016/01/07/texture-classification/
- http://joelcarlson.github.io/2015/07/10/radiomics-package/

Configuring Texture Feature Tool via R-ArcGIS Bridge

Download and Install R and RStudio

1. Download R from: http://cran.us.r-project.org/ and follow installation instructions
2. Download RStudio from https://www.rstudio.com/products/rstudio/download/#download

Download and Configure R-ArcGIS Bridge

- Download and follow instructions from https://github.com/R-ArcGIS/r-bridge-install
- Additional: https://learn.arcgis.com/en/projects/analyze-crime-using-statistics-and-the-r-arcgis-bridge/

Adding Texture Feature R script to Toolbox

1) Create a new toolbox in the Project folder
2) Add Script, leaving default parameter properties except for Direction, set according to the table below

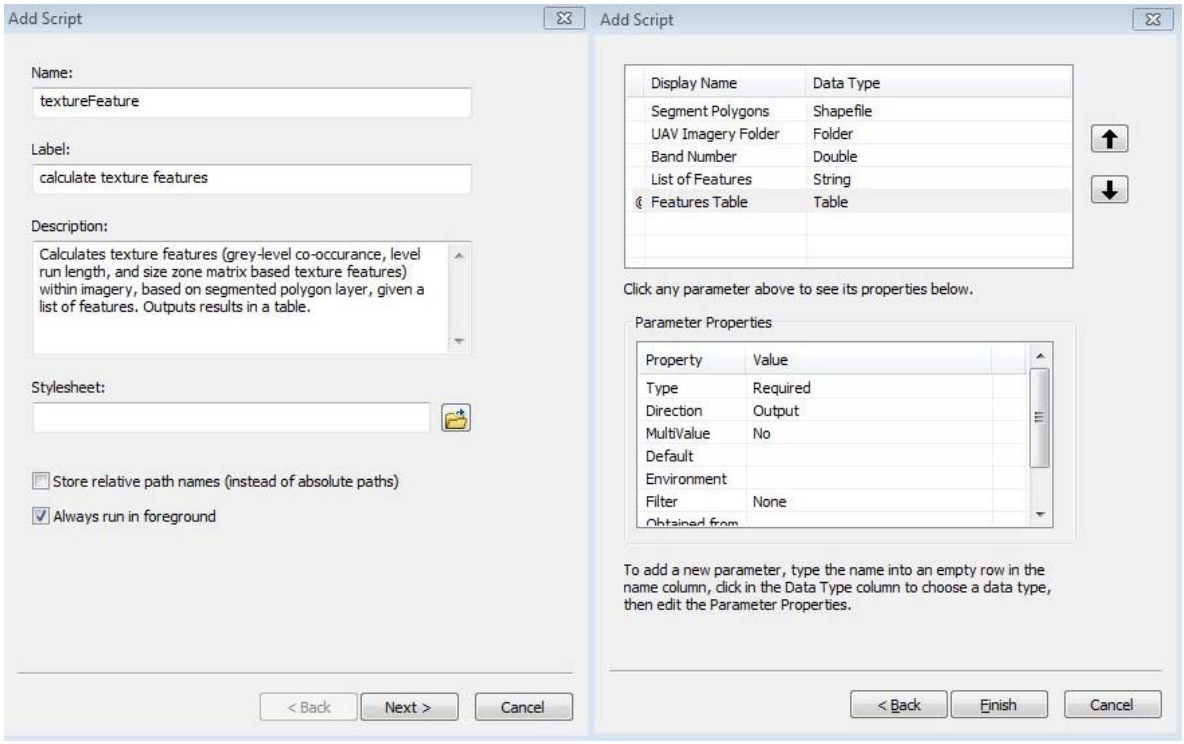

Direction	Display Name	Data Type
Input	Segment Polygon	Shapefile
Input	UAV Imagery Folder	Folder
Input	Number Band	Double
Input	Comma-separated List of Features	String
Output	Feature Table	Table

Using the Texture Feature Toolbox to Generate Texture Feature Layers

- Create shapefile with polygon segments and unique and sequential integer IDs stored in variable called "POLY_ID" which will be used in matching the texture feature values to their original polygons in the shapefile so tables can be used to generate raster layers to add to image classification workflow
- Inspect segmentation layer output to confirm correct level of detail, and check for and remove fragments smaller than about 10 original raster pixels before assigning the POLY_IDs
- Run the Texture Feature Tool on one band at a time; note that UAV imagery must be stored in its own folder, with bands each as individual rasters in a format able to be read by R's raster package (all standard raster formats; see raster documentation)
- List of Features must be given as a list separated by commas with glcm_, glrlm_, or glszm_ preceding the feature abbreviation as given in Table 2 below
- Table output must be saved to a file geodatabase

First Order	GLCM	GLRLM	GLSZM
energy	mean	GLN	SAE
entropy	variance	HGLRE	LAE
kutosis	autoCorrelation	LRE	IV
meanDeviation	cProminence	LRHGLE	SZV
skewness	cShade	LRLGLE	ZP
uniformity	cTendancy	LGLRE	LIE
mean	contrast	RLN	HIE
median	correlation	RP	LISAE
max	differenceEntropy	SRE	HISAE
min	dissimilarity	SRHGLE	LILAE
diff	energy	SRLGLE	HILAE
var	entropy		
RMS	homogeneity1		
sd	homogeneity2		
	IDMN		
	IDN		
	inverseVariance		
	maxProb		
	sumAverage		
	sumEntropy		
	sumVariance		

APPENDIX 8. R scripts for texture feature calculation and analysis.

The texture analysis we coded in the R script takes a polygon layer, a folder containing the grey-scale rasters, the name of the single-band raster file to be used, and a comma separated string of features to calculate as inputs. The tool identifies portions of the raster UAV imagery that overlap each polygon, creates matrices that fill the non-overlapping portions of the square with NA, calculates their grey-level co-occurrences, and then the specified texture features. The output is given as an ArcGIS table. The R-ArcGIS bridge works by transporting data into R, conducting an analysis in R, and then transporting the results back to ArcGIS. This is advantageous because it circumvents the 32-bit constraints of ArcGIS Desktop.

```
tool_exec <- function(in_params, out_params)
{
  cat(paste0("\n", "Loading packages...", "\n"))
  # load required packages and install if needed
  if (!requireNamespace("radiomics", quietly = TRUE))
    install.packages("radiomics")
  if (!requireNamespace("raster", quietly = TRUE))
    install.packages("raster")
  if (!requireNamespace("sp", quietly = TRUE))
    install.packages("sp")
  pkgs <- c("radiomics", "raster", "sp", "doParallel", "foreach", "rgdal", "compiler")
  lapply(pkgs, require, character.only = TRUE)

  cat(paste0("\n", "Loading datasets...", "\n"))
  # read input and output parameters
  segment_polygons = in_params[[1]]
  image_folder = in_params[[2]]
  band_name = in_params[[3]]
  feature_str = in_params[[4]]
  out_table = out_params[[1]]

  # read segmented polygon layer and single band of image from rasters folder
  polygonlist <- arc.data2sp(arc.select(arc.open(segment_polygons)))
  num_polygons <- as.numeric(length(polygonlist@data$POLY_ID))
  img <- raster(paste(image_folder, band_name, sep = "/"))

  # identify from input character string which features to are to be calculated
  features <-  strsplit(feature_str, ", ")[[1]]
  glcm_ft <- grep("^glcm", features, value = TRUE); glrlm_ft <- grep("^glrlm", features, value = TRUE); glszm_ft <- grep("^glszm", features, value = TRUE); firstOrder_ft <- grep("^calc", features, value = TRUE)
  glcm_bool <- length(glcm_ft)!=0; glrlm_bool <- length(glrlm_ft)!=0; glszm_bool <- length(glszm_ft)!=0; firstOrder_bool <- length(firstOrder_ft)!=0

  cat(paste0("\n", "Compiling texture feature calculation functions...", "\n"))
  # create compiled functions to speed texture feature calculations
  cmp_glcm <- cmpfun(function(x) as.numeric(calc_features(glcm(as.matrix(rasterize(x, crop(img, extent(x)), mask = TRUE)), n_grey = 128), glcm_ft)))
  cmp_glrlm <- cmpfun(function(x) as.numeric(calc_features(glrlm(as.matrix(rasterize(x, crop(img, extent(x)), mask = TRUE)), n_grey = 128), glrlm_ft)))
  cmp_glszm <- cmpfun(function(x) as.numeric(calc_features(glszm(as.matrix(rasterize(x, crop(img, extent(x)), mask = TRUE)), n_grey = 128), glszm_ft)))
  cmp_1stOrd <- cmpfun(function(x) as.numeric(calc_features(as.matrix(rasterize(x, crop(img, extent(x)), mask = TRUE)), firstOrder_ft)))

  cat(paste0("\n", "Calculating texture features...", "\n"))
  # parallelize and calculate texture features
  cores <- detectCores()-1
  cl <- makeCluster(cores)
  registerDoParallel(cl)
  vec <- vector(length = length(features)+1)
  featureVals <- foreach(i = polygonlist@data$POLY_ID, .packages= c("radiomics","raster","foreach"), .combine = cbind) %dopar% {
    vec[1] <- i
    if(glcm_bool) vec[2:(length(glcm_ft)+1)] <- cmp_glcm(polygonlist[polygonlist@data$POLY_ID == i,])
    if(glrlm_bool) vec[(length(glcm_ft)+2):(length(glcm_ft)+length(glrlm_ft)+1)] <- cmp_glrlm(polygonlist[polygonlist@data$POLY_ID == i,])
    if(glszm_bool) vec[(length(glcm_ft)+length(glrlm_ft)+2):(length(glcm_ft)+length(glrlm_ft)+length(glszm_ft)+1)] <- cmp_glszm(polygonlist[polygonlist@data$POLY_ID == i,])
    if(firstOrder_bool) vec[(length(glcm_ft)+length(glrlm_ft)+length(glszm_ft)+2):(length(features)+1)] <- cmp_1stOrd(polygonlist[polygonlist@data$POLY_ID == i,])
    featureVals <- vec
  }
  stopCluster(cl)
  closeAllConnections()

  cat(paste0("\n", "Writing result datasets...", "\n"))
  # export textures features output array
  band <- substr(band_name, 1, nchar(band_name)-4)
  texture_features <- as.data.frame(t(featureVals))
  colnames(texture_features) <- c("POLY_ID", paste(features, band, sep = "_"))
  if (!is.null(out_table) && out_table != "NA")
    arc.write(out_table, texture_features)
  cat(paste0("\n", "Done.", "\n"))
  return(out_params)
}
```

```
tool_exec <- function(in_params, out_params)
{
  cat(paste0("\n", "Loading packages...", "\n"))

  # load required packages and install if needed
  if (!requireNamespace("mclust", quietly = TRUE))
    install.packages("mclust")
  require(mclust)

     # read input and output parameters
  training_data_in = in_params[[1]]
  presence_varname = in_params[[2]]
  feature_str = in_params[[3]]
  predict_data_in = in_params[[4]]
  out_table = out_params[[1]]

  # read training data and segmented polygon layers as tables
  training_data <- arc.select(arc.open(training_data_in))
  all_data <- arc.select(arc.open(predict_data_in))

  # identify from input character string which features to are to be used in classifying
  features <-  strsplit(feature_str, ", ")[[1]]

  cat(paste0("\n", "Fitting model and predicting...", "\n"))

  classes <- training_data[,presence_varname]
  trdata_subset <- training_data[, features]
  mclustMod <- MclustDA(trdata_subset, classes)
  predict_data <- all_data[, features]
  predictions <- predict(mclustMod, predict_data)
  predictions_df <- as.data.frame(predictions)

  cat(paste0("\n", "Writing result datasets...", "\n"))

  # export model predictions (z-scores) to a table
  zscores_table <- data.frame(all_data[,"POLY_ID"], predictions_df)
  colnames(zscores_table) <- c("POLY_ID", colnames(predictions_df))

  if (!is.null(out_table) && out_table != "NA")
    arc.write(out_table, zscores_table)

  cat(paste0("\n", "Done.", "\n"))
  return(out_params)
}
```

APPENDIX 9. Texture analysis workflow.

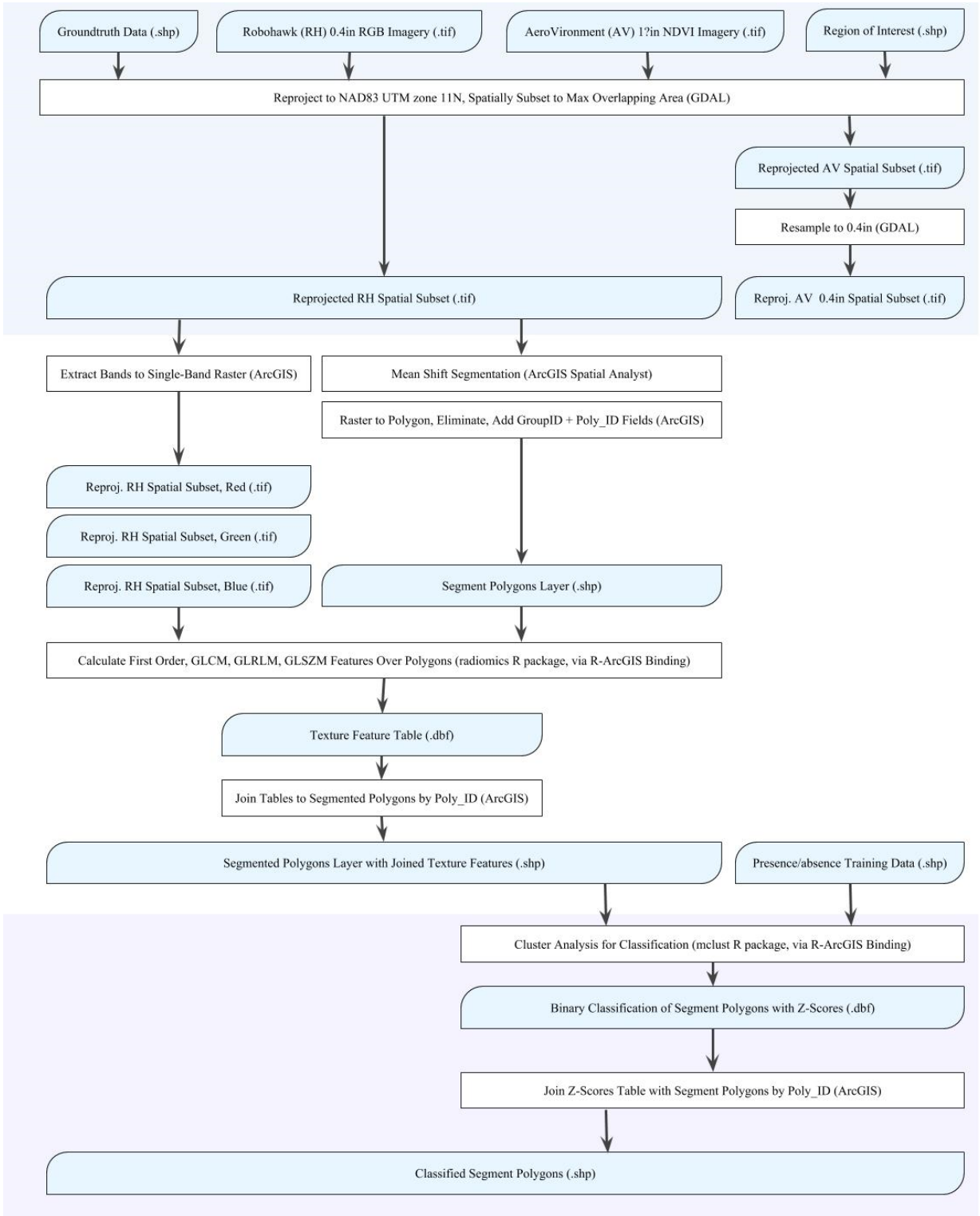

APPENDIX 10. Inputs into the cost benefit analysis.

Option 1. Drone purchase

	COSTS										BENEFIT	Discounted	NPV of Cash
Year	Drone	Neutral Density Filter	Case	Imaging software	Pilot Certification	Registration	Sensors	MicroSD	Batteries	Insurance/repair package		Benefit	Flow
0	$ 1,200.00	$30.00	$250.00	$ 1,000.00	$ 150.00	$ 5.00	$ 2,100.00	$ 68.00	$ 507.00	$ 140.00	$ 3,240.00	$3,240.00	$ (2,210.00)
1	$ -	$ -	$ -	$ 1,000.00	$ -	$ -	$ -	$ 68.00	$ 507.00	$ 140.00	$ 3,240.00	$3,028.04	$ 1,425.23
2	$ -	$ -	$ -	$ 1,000.00	$ 150.00	$ -	$ -	$ 68.00	$ 507.00	$ 140.00	$ 3,240.00	$2,829.94	$ 1,200.98
3	$ -	$ -	$ -	$ 1,000.00	$ -	$ -	$ -	$ 68.00	$ 507.00	$ 140.00	$ 3,240.00	$2,644.81	$ 1,244.85
4	$ -	$ -	$ -	$ 1,000.00	$ 150.00	$ -	$ -	$ 68.00	$ 507.00	$ 140.00	$ 3,240.00	$2,471.78	$ 1,048.98
5	$ -	$ -	$ -	$ 1,000.00	$ -	$ -	$ -	$ 68.00	$ 507.00	$ 140.00	$ 3,240.00	$2,310.08	$ 1,087.30
	$ 1,200.00	$ 30.00	$ 250.00	$ 6,000.00	$ 450.00	$ 5.00	$ 2,100.00	$ 408.00	$ 3,042.00	$ 840.00	$ 19,440.00		

			Total Cost	$ 14,325.00		BCR	1.153552509		NPV	$ 3,797.35			
			Total Benefit	$ 16,524.64									

Option 2. Contract drone service

	COSTS	BENEFIT	Discounted	NPV of Cash
Year	Service		Benefit	Flow
0	$ 18,000.00	$ 3,240.00	$3,240.00	$ (14,760.00)
1	$ 18,000.00	$ 3,240.00	$3,028.04	$ (13,794.39)
2	$ 18,000.00	$ 3,240.00	$2,829.94	$ (12,891.96)
3	$ 18,000.00	$ 3,240.00	$2,644.81	$ (12,048.56)
4	$ 18,000.00	$ 3,240.00	$2,471.78	$ (11,260.33)
5	$ 18,000.00	$ 3,240.00	$2,310.08	$ (10,523.68)
	$ 108,000.00	$ 19,440.00	$ 16,524.64	$ (75,278.91)

Total Cost	$ 108,000.00
Total Benefit	$ 33,049.28
BCR	0.3060118462
NPV	$ (150,557.83)

APPENDIX 11. Discriminant analysis model summary.

```
------------------------------------------------
Gaussian finite mixture model for classification
------------------------------------------------

MclustDA model summary:

 log.likelihood   n  df       BIC
      -4632.52 233 859 -13947.48

Classes   n Model G
      0 173   VEV 4
      1  60   VEV 5

Training classification summary:

     Predicted
Class   0   1
    0 147  26
    1   9  51

Training error = 0.1502146
```

APPENDIX 12. Further applications of UAS technology and justification for image classification techniques.

Detecting Conifer Tree Stress and Morality

Detection of tree stress and mortality from satellite imagery typically uses phenotypic traits such as brightness, greenness, or wetness (Ferrell et al., 1993; Meddens et al., 2013; Coops et al., 2006). Generally, results are more accurate at higher levels of tree mortality, or in "red attack" stage when needles change color a few years after infestation (Hicke & Logan, 2009; Meddens et al., 2013; Coops et al., 2006). Meddens et al. found, using a time-series of 20 30-meter spatial resolution Landsat images taken between 1996 and 2011, a multi-date method was more accurate at detecting intermediate levels of red-stage mortality (Meddens et al., 2013). The methods were found to be useful for detecting severe insect disturbance (i.e., killing> ~25% of trees in the canopy within a pixel), but not for detecting dispersed tree mortality (i.e., single trees) across the forested landscapes (Meddens et al., 2011). Coops et al. used single-date QuickBird (2.5 m spatial resolution) imagery to classify pixels containing red attack damage using methods incorporating Normalized difference vegetation index (NDVI) and a red-green index (RGI), both found to be significant predictors (Coops et al., 2006).

Detection of Other Invasive Plant Species from Satellite and Aerial Imagery

There have also been studies on the detection and mapping of other invasive species including Sahara mustard (*Brassica tournefortii*), yellow starthistle (*Centaurea solstitialis*), and perennial pepperweed (*Lepidium latifolium*) (Nguyen et al., 2012; Lass et al., 2005; Lass et al., 2000; Ge et al., 2007; Lawrence et al., 2005). Classifications using high spectral resolution imagery from sensors like AVIRIS, CASI-II, EO-1 Hyperion, or ASTER, especially when combined with environmental variables have achieved accuracies of 70-80% (Ge et al., 2007; Nguyen et al., 2012; Zhang & Xie, 2012). Margaret Andrew and Susan Ustin mapped perennial pepperweed (*Lepidium latifolium*) at three sites in California using 3-meter spatial resolution, 128-band HyMap imagery, with aggregated classification and regression tree models (CART) incorporating mixture tuned matched filter (MTMF) results – which essentially indicate how likely a pixel is to be each endmember – and spectral physiological indexes including NDVI and cellulose absorption index (CAI) (Andrew & Ustin, 2008). Detection was successful only at two of the three sites, however, highlighting the importance of environmental context that allows spectral and/or phenological distinction of the target species (Andrew & Ustin, 2008).

Object-Based Image Processing

One study found that in classification of 5cm-resolution UAV-acquired imagery of arid rangeland with shrubs, grasses, and bare soils, inclusion of texture derivatives resulted in significantly higher overall accuracy; optimal texture features as determined by a previous study included entropy, contrast, and standard deviation (Laliberte & Rango, 2008). Another study with similar findings used 7cm-resolution imagery and grass, trees, shrubs as the three vegetated categories, and six least-correlated textures derived from gray-level co-occurrence matrices (GLCM): mean, standard deviation, homogeneity, dissimilarity, entropy, and angular second moment (Feng et al., 2015; Szantoi et al., 2013).

APPENDIX 13. Further examples of imaging methods.

In order for these mosaic maps to be useful for land managers in the context of invasive vegetation, they must be able to rapidly and confidently discern them from native species. Thus, automated classification algorithms require the inclusion of spectral emission data in the near infrared wavelength band. This data is a proxy of variable chlorophyll levels and can inform classification algorithms of spectrally unique plant classes and species. Using the "RandomForest" package for the open-source data analysis software RStudio, Michez and colleagues were able to map a riparian habitat and autonomously identify three invasive weeds with 72-97% accuracy using the additional NIR band (Michez et al., 2016). The random forest classification method can be applied to large data sets with training classes to semi-autonomously classify test groups into representative training categories. It is called a random forest because it utilizes a vast amount of branching decision trees to compare and identify the most discriminating feature variables.

Similarly, Oumer Ahmed's research group classified vegetation with a random forest package found in the remote sensing software ENVI but used Pix4D for image mosaicking (Ahmed at al., 2017). Using the multi-spectral Parrot Sequoia camera, an Australian group was able to classify vegetation cover classes with accuracies in excess of 70% (Strecha et al., 2012). Led by Christoph Strecha, Pix4D was also used to generate stitched mosaics, however, a maximum likelihood supervised classification tool was run in the remote sensing software ERDAS (Strecha et al., 2012). The maximum likelihood classification tool attempts to group data sets in the most probabilistically likely category based on defined spectral variables. Strecha's group was able to extract certain vegetation species but found that object-based image classification may yield better results in areas without distinct contrasting flower pigmentation (Strecha et al., 2012).

APPENDIX 14. Abridged list of satellite and aerial imagery sources and specifications.

	NAIP (NDOP)	AVIRIS	AVIRIS NG (Next Generation)
Operating Entity	USDA, FSA	NASA, JPL	NASA, JPL
Coverage	US	Tasking, with coverage of most of Tejon	No current coverage of Tejon
Operational Lifetime	Ongoing	Depends on funding	Depends on funding
Instrument/Sensor	RGB-NIR	Imaging Spectrometer	Imaging Spectrometer
Spatial Resolution	50 - 60 cm in California	15.3 m over Tejon	4 m
Temporal Resolution	Three year cycle, since 2009	Each June, for the past 5 years	N/A
Available How Soon	CCMs within 2 months, DOQQs within a year	48-72 hours after collection	48-72 hours after collection
Number of Bands	4	224	481
Approximate Spectral Range	380 - 950 nm	400 - 2500 nm	380 - 2510 nm
Relative Spectral Responses	Varies by vendor	Approximately 10 nm wide	Approximately 5 nm wide
Community/Online Support	Decent	Good	Decent
File Format(s)	DOQQs, CCM	.tar file with img files	.tar file with img files
Projection/Datum	UTM NAD83	WGS-84 UTM zone 11	WGS-84 UTM zone 11
Spatial Accuracy	Horizontal accuracy within six meters of photo-identifiable ground control points,	<10 for low altitude flights, greater for higher altitude flights and dependant on conditions	<10 for low altitude flights, greater for higher altitude flights and dependant on conditions
Additional Details	Less than 10% cloud cover per quarter quad tile	Orthocorrected upwelling radiance radiometrically calibrated to less than 10% absolute	Orthocorrected and atmospherically corrected reflectance data

	Landsat 8 OLI	Landsat 8 TIRS	ASTER	MODIS	VIIRS	Sentinel-2 MSI	GOES-R ABI	RapidEye	4-band PlanetScop
Operating Entity	USGS, NASA	USGS, NASA	NASA, Japan METI	NASA	NOAA, NASA	ESA	NOAA, NASA	Planet	Planet
Operational Lifetime	May 2013, ongoing	May 2013, ongoing	Ongoing	Ongoing	Nov 2011, ongoing, one in a series of 4 planned	March 2017, seven years planned	One in a series of 4 planned through 2036	Ongoing	Ongoing
Spatial Resolution	30 m, 15 m panchromatic	100 m, resampled to 30 m	15 m VNIR, 30 m SWIR, 90 m TIR	250 m (bands 1-2), 500 m (3-7), 1000 m (8-36)	16 bands with 750 m, 5 bands with 375 m	Four bands at 10 m, six at 20 m, three at 60 m	500 m for 640 nm, 1 km other visible, 2 km IR	6.5 m	3.2 m
Temporal Resolution	16 day revisit cycle	16 day revisit cycle	16 day revisit cycle	1-2 day revisit cycle	Full coverage every 12 hr	5 day revisit cycle	Daily	Daily	Daily
Available How Soon	Within 24 hours	Within 24 hours	Typically 5 days	Level 1 data available within 2 days	Level 1 data available within 2 days	10 - 15 days	Level 1 within 24 hours	2 weeks after collection through Open California program	2 weeks after collection through Open California program
Number of Bands	8	2	15	36	22	13	16	5	4
Approximate Spectral Range	435 - 1384 nm	10600 - 12510 nm	520 - 1165 nm	405 - 14385 nm	412 - 12010 nm		470 - 13300 nm	380 - 950 nm	380 - 950 nm
Community/Online Support	Very good	Very good	Good	Very good	Very good	Very good	Good	Very good	Very good
File Formats	GeoTIFF, JPG, PNG, BMP	GeoTIFF	HDF-EOS	HDF-EOS	HDF-EOS5	JPEG2000	NetCDF	GeoTIFF	Ortho Tile
Projection/Datum	UTM WGS84	UTM WGS84	UTM WGS84	Sinusoidal projection with WGS84	Sinusoidal projection with WGS84	UTM/WGS84		UTM WGS84	UTM WGS84
Spatial Accuracy	<10m	<10m	4%	<45m	<60m	<12.5m		<10m	<10m
Additional Details	Radiometrically calibrated, orthorectified using ground control points and DEM, surface reflectance available	Radiometrically calibrated, orthorectified using ground control points and DEM, surface reflectance available	Level 1 Precision Terrain Corrected Registered At-Sensor Radiance	Surface reflectance, corrected for atmospheric gases and aerosols, with best possible observation during 8-day period	Successor to MODIS	TOA reflectances in fixed cartographic geometry, bottom of atmosphere reflectances can be generated using Sentinel-2 Toolbox	Many available products; level 1b radiometrically corrected radiances, cloud and moisture products, total precipitable water,	Orthocorrected using GCPs and 30-90m DEM to <10m RMSE positional accuracy, conversion to absolute radiometric values	Orthorectified using GCPs and 30-90m DEM to <10m RMSE positional accuracy, no radiometric calibration
Instrument/Sensor	Multispectral	Thermal Infrared Sensor	Thermal Emission & Reflection Radiometer	Moderate-Resolution Imaging Spectroradiometer	Visible Infrared Imaging Radiometer Suite	Multi-Spectral Instrument	Advanced Baseline Imager (Multispectral)	Multispectral	Multispectral
Platform	Landsat 8	Landsat 8	Terra	Terra and Aqua	JPSS-1	Twin polar-orbiting satellites	Geostationary Operational Environmental Satellite	Satellite constellation	Satellite constellation
Spectral Responses	https://landsat.gsfc.nasa.gov/operational-land-imager-oli/	https://landsat.gsfc.nasa.gov/preliminary-spectral-response-of-the-thermal-infrared-sensor/	https://asterweb.jpl.nasa.gov/characteristics.asp	https://modis.gsfc.nasa.gov/about/specifications.php	https://ladsweb.modaps.eosdis.nasa.gov/missions-and-measurements/viirs/	https://sentinel.esa.int/web/sentinel/missions/sentinel-2/instrument-payload/resolution-and-swath	https://www.goes-r.gov/education/ABI-bands-quick-info.html	55-70nm for RGB, 90nm for NIR	60-90nm

APPENDIX 15. Traceability matrix

SCIENCE		MEASUREMENT
Monitoring Category	**Conservation Questions**	**Observable (Remote or Field) Physical Features**
Invasive Plant Species: Presence, hotspots and other patterns of patial distribution, abundance, spread.	What invasive plant species are present? Where are invasive plants currently located? How abundant are certain invasive species overall? In locations where present, what is the density of the species of concern? Where have invasive species spread through time? How effective have invasive weed management activities been? What changes in area covered and vegetation types are occuring over time?	Variation in climatic and environmental characteristics including soil moisture, mean temperature, precipitaion. Terrain variables includeing slope, aspect, elevation, proximity to streams. Soil type Species-level and vegetation community-level spectral signatures, i.e. radiance in key wavelengths and differentials between them Spatially distinct patches of different vegetation types Decreased NDVI due to vegetation die-back Moisture levels over time Phenology, i.e. changes in spectral signatures or textures over time due to seasonal changes in plants Texture of vegetation and land cover Canopy height
Conservation Easement Compliance: Current noncompliance, locations of infractions, types of infractions	What is the current compliance status of each conservation easement? Are cattle grazing in acceptable locations?	Impermeable surfaces or structures New soil deposits or new water bank areas Major change in vegetation cover Pasture color changes, not associated with phenology Cattle drive or corral locations Fence lines
Conifer Health: Health status of conifers, extent and severity of conifer mortality, cause of stress or mortality	What is the mortailty rate of conifers? How many are dead (increases in canopy area of dead trees)? How can the Conservancy monitor or track bark beetle infestation? What is the health of conifers? Where is conifer mortality or stress occurring? What is the stress level of conifers on the ranch?	Spatially distinct stands of different tree types Spectral signatures of healthy, conifers stressed by drought, and conifers stressed by bark beetle pests Density of canopy cover Canopy height Variation in climatic and environmental characteristics including soil moisture, mean temperature, precipitaion. Terrain variables includeing slope, aspect, elevation, proximity to streams. Soil type

	MEASUREMENT		
	Observable (Remote or Field) Physical Features	**Objective & Measurement Parameters**	**Instrument or Data Source**
	Variation in climatic and environmental characteristics including soil moisture, mean temperature, precipitaion.	Link environmental variables -- which may dictate suitablility or preferred characteristics for species habitat -- to likelihood of invasive species presence. 10m resolution for terrain variables, 0.5km for climatic.	CalCommons: California Landscape Conservation Cooperative, or
	Terrain variables includeing slope, aspect, elevation, proximity to streams.		National elevation dataset (NED)
	Soil type		State Soil Geographic (STATSGO2)
	Species-level and vegetation community-level spectral signatures, i.e. radiance in key wavelengths and differentials between them	Characterize full spectral signatures of invasive species, radiometric errors <5%, at spatial resolution fine enough that signal-to-noise ratio sufficient for detecting individual plant species.	Quadcopter with RGB+NIR sensor capabilities or UAV with lightweight imaging spectrometer
		Create phenologic calendars of invasives and of dominant native species, via groundtruthed "image library" of species, in order to be able to separate changes in spectra due to phenology from those associated with changes species composition. Plant size, foliage and flower color, flowering or not, etc.	
		Characterize spectral sigatures of native, uninvaded vegetation communities, with radiometric errors <10%	
			Landsat 8
	Spatially distinct patches of different vegetation types	Identify spatially distinct patches of invasive species. Spatial resolution 4m or better	Planet.com PlanetScope, or UAV RGB e.g. DJI Phantom 4 Advanced
	Decreased NDVI due to vegetation die-back	Measure success of weed management strageties by assessing health of managed patches of invasive species, via NDVI. Spatial resolution on par with mean size of plant individuals or groups being monitored, about 4m	Planet.com PlanetScope, or UAV RGB+NIR e.g. DJI Phantom 4 Advanced with NIR sensor upgrade
	Moisture levels over time	Assess if invasive species e.g. tamarisk are altering local hydrology or soil resources. Spatial resolution ~1km, measurement error <10%.	SMAP (3km), Sentinel-1 (1km)
	Phenology, i.e. changes in spectral signatures or textures over time due to seasonal changes in plants	Create phenologic calendars of invasives and of dominant native species, via groundtruthed "image library" of species, in order to be able to separate changes in spectra and texture due to phenology from those associated with changes species composition. Spatial resolution fine enough that signal-to-noise ratio sufficient to resolve plants.	Quadcopter with RGB+NIR sensor capabilities or UAV with lightweight imaging spectrometer
	Texture of vegetation and land cover		UAV RGB e.g. DJI Phantom 4 Advanced
	Canopy height	Measure canopy height, within 10cm vertical accuracy, and with horizontal resolution 10-100cm	UAV-based or aircraft-based lidar
	Impermeable surfaces or structures	Determine if structures are being built on conserved lands. Imagery with infrared band, to help discriminate between vegetation, water bodies, and impervious surfaces. Spatial resolution <10m.	Planet.com RapidEye, or UAV RGB+NIR e.g. DJI Phantom 4 Advanced with Near Infrared sensor upgrade
	New soil deposits or new water bank areas		
	Major change in vegetation cover	Identify areas of major vegetation change e.g. illegal farming or timber harvest activity	
		Assess impact of intensive cattle/grazing activity	
	Pasture color changes, not associated with phenology		UAV RGB e.g. DJI Phantom 4 Advanced
	Cattle drive or corral locations		
	Fence lines		
	Spatially distinct stands of different tree types	Assess overall health over conifer stands using NDVI	Planet.com RapidEye
	Spectral signatures of healthy, conifers stressed by drought, and conifers stressed by bark beetle pests	Use NDVI and other vegetation indices to distinguish red-attack or earlier phases of beetle infestation of within conifer stands	Sentinel-2
			Landsat 8
	Density of canopy cover	Estimate area coverage of conifers within larger pixels of Landsat or Sentinel imagery, via photogrammetric image processing tools or with lidar imagery	UAV RGB+NIR e.g. DJI Phantom 4 Advanced with Near Infrared sensor upgrade
	Canopy height	Measure canopy height and foliage density, within 1m vertical accuracy, and with horizontal resolution 10-100cm	UAV-based or aircraft-based lidar
	Variation in climatic and environmental characteristics including soil moisture, mean temperature, precipitaion.	Determine if there are significant factors besides spatial proximity to previously infected stands, that influence direction and rates of infection	CalCommons: California Landscape Conservation Cooperative, or WorldClim: Global Climate Data
	Terrain variables includeing slope, aspect, elevation, proximity to streams.		National elevation dataset (NED)
	Soil type		State Soil Geographic (STATSGO2)

Literature Cited

Ecological Monitoring with UAVs

Ahmed, Oumer S., et al. “Hierarchical Land Cover and Vegetation Classification Using Multispectral Data Acquired from an Unmanned Aerial Vehicle.” AGRIS: International Information System for the Agricultural Science and Technology, Taylor & Francis, 1 Jan. 2017, agris.fao.org/agris-search/search.do?recordID=US201700084286.

Anderson, Karen, and Kevin J Gaston. “Lightweight Unmanned Aerial Vehicles Will Revolutionize Spatial Ecology.” Frontiers in Ecology and the Environment, vol. 11, no. 3, 2013, pp. 138–146., doi:10.1890/120150.

Breckenridge, Robert P., et al. “Comparison of Unmanned Aerial Vehicle Platforms for Assessing Vegetation Cover in Sagebrush Steppe Ecosystems.” Rangeland Ecology & Management, vol. 64, no. 5, 2011, pp. 521–532. doi:10.2111/rem-d-10-00030.1.

“BioCarbon Engineering: Industrial-Scale Ecosystem Restoration.” BioCarbon Engineering: Industrial-Scale Ecosystem Restoration, 2018, www.biocarbonengineering.com/.

Cruzan, Mitchell B., et al. “Small Unmanned Aerial Vehicles (Micro-UAVs, Drones) in Plant Ecology.” Applications in Plant Sciences, vol. 4, no. 9, 2016, p. 1600041., doi:10.3732/apps.1600041.

Dehaan, Remy, et al. “The Design and the Development of a Hyperspectral Unmanned Aircraft Mapping System for the Detection of Invasive Plants.” Charles Sturt University, Weed Society of Victoria Inc., 2012, researchoutput.csu.edu.au/en/publications/the-design-and-the-development-of-a-hyperspectral-unmanned-aircra.

Gonzalez, Luis, et al. “Unmanned Aerial Vehicles (UAVs) and Artificial Intelligence Revolutionizing Wildlife Monitoring and Conservation.” Sensors, vol. 16, no. 1, 2016, p. 97., doi:10.3390/s16010097.

Ivosevic, Bojana, et al. “Calculating Coniferous Tree Coverage Using Unmanned Aerial Vehicle Photogrammetry.” Journal of Ecology and Environment, vol. 41, no. 1, 2017, doi:10.1186/s41610-017-0029-0.

Lu, Bing, and Yuhong He. “Species classification using Unmanned Aerial Vehicle (UAV)-acquired high spatial resolution imagery in a heterogeneous grassland.” Photogrammetry and Remote Sensing, vol. 128, 2017, pp. 73-85. doi: 10.1016/j.isprsjprs.2017.03.011.

Mafanya, Madodomzi, et al. “Evaluating pixel and object based image classification techniques for mapping plant invasions from UAV derived aerial imagery: *Harrisia pomanensis* as a case study.” *ISPRS Journal of Photogrammetry and Remote Sensing*, vol. 129, 2017, pp. 1-11. doi:10.1016/j.isprsjprs.2017.04.009.

Michez, Adrien, et al. “Mapping of Riparian Invasive Species with Supervised Classification of Unmanned Aerial System (UAS) Imagery.” International Journal of Applied Earth Observation and Geoinformation, vol. 44, 2016, pp. 88–94. doi: 10.1016/j.jag.2015.06.014.

Rango, Albert, et al. “Unmanned Aerial Vehicle-Based Remote Sensing for Rangeland Assessment, Monitoring, and Management.” Journal of Applied Remote Sensing, vol. 3, no. 1, Jan. 2009, p. 033542. doi: 10.1117/1.3216822.

Strecha, C., et al. “Developing Species Specific Vegetation Maps Using Multi-Spectral Hyperspatial Imagery From Unmanned Aerial Vehicles.” ISPRS Annals of Photogrammetry, Remote Sensing and Spatial Information Sciences, I-3, 2012, pp. 311–316. doi: 10.5194/isprsannals-i-3-311-2012.

Tamouridou, A. A., et al. “Evaluation of UAV Imagery for Mapping Silybum Marianum weed Patches.” International Journal of Remote Sensing, June 2016, pp. 1–14. doi: 10.1080/01431161.2016.1252475.

Unmanned Aerial Systems & Software

"Computer Requirements." Pix4D Computer Requirements, 2018, support.pix4d.com/hc/en-us/articles/115002495966-Computer-requirements#gsc.tab=0.

"Downloads System Requirements." Agisoft Photoscan System Requirements, 2018, www.agisoft.com/downloads/system-requirements/.

"FAA Regulations Part 107." 14 CFR PART 107—SMALL UNMANNED AIRCRAFT SYSTEMS , Federal Aviation Administration, 2016, avsport.org/UAS/ground/PART%20107.pdf.

"Home." DroneSeed, 2017, www.droneseed.co/.

"License Package Pricing." Pricing & Plans for Pro Business and Enterprise | DroneDeploy, www.dronedeploy.com/pricing.html.

"The DJI Store: Shop for World-Class Drones and Gimbals." DJI Store, 2018, store.dji.com/.

United States. Department of Transportation. Volpe National Transportation Systems Center. Small Unmanned Aircraft and the U.S. Forest Service : Benefits, Costs, and Recommendations for Using Small Unmanned Aircraft in Forest Service Operations. N.p.: n.p., 2016. Print.

"Yuneec Aerial Drones." Drones, 2017, us.yuneec.com/.

Monitoring Conifer Tree Health via Satellite Imagery

Bright, B. C., J. A. Hicke, and A. J. H. Meddens. "Effects of bark beetle-caused tree mortality on biogeochemical and biogeophysical MODIS products." Journal of Geophysical. Research. Biogeoscience, vol. 118, 2013, pp. 974–982. doi:10.1002/jgrg.20078.

Eitel, Jan U.H., et al. "Broadband, red-edge information from satellites improves early stress detection in a New Mexico conifer woodland." Remote Sensing of Environment, vol. 115, no. 12, December 2011, pp. 3640-3646. doi:10.1016/j.rse.2011.09.002.

Ferrell, G. T, W.J. Otrosina, and C.J. DeMars. "Predicting susceptibility of white fir during a drought-associated outbreak of fir engraver, *Scolytus ventralis*, in California." The Canadian Entomologist, vol. 125, September 1993, pp. 895-901. doi:10.1139/x94-043.

Hicke, Jeffrey A., and Jesse Logan. "Mapping whitebark pine mortality caused by a mountain pine beetle outbreak with high spatial resolution satellite imagery." International Journal of Remote Sensing, vol. 30, 2009, pp. 4427-444104. doi:10.1080/01431160802566439.

Meddens, Arjan, Jeffrey A. Hicke, Lee Vierling, and AT Hudak. "Evaluating methods to detect bark beetle-caused tree mortality using single-date and multi-date Landsat imagery." Remote Sensing of Environment, vol. 132, pp. 49–58. doi:10.1016/j.rse.2013.01.002.

Meddens, Arjan J.H., Jeffrey A. Hicke, and Lee A. Vierling. "Evaluating the potential of multispectral imagery to map multiple stages of tree mortality." Remote Sensing of Environment, vol. 115, no. 7, 2011, pp. 1632-1642. doi:10.1016/j.rse.2011.02.018.

Näsi, Roope, et al. "Using UAV-Based Photogrammetry and Hyperspectral Imaging for Mapping Bark Beetle Damage at Tree-Level." Remote Sensing, vol. 7, no. 11, 2015, pp. 5467-15493. doi:10.3390/rs71115467.

Ortiz, Sonia, Johannes Breidenbach, and Gerald Kändler. "Early detection of Bark beetle green attack using TerraSAR-X and RapidEye Data." Remote Sensing, vol. 5, issue 4, 2013, pp. 1912-1931. doi:10.3390/rs5041912.

Vegetation Mapping and Detection via Satellite Imagery

Dabrowska-Zielinska, Katarzyna, et al. “Monitoring Wetland Ecosystems Using ALOS PALASAR (L-Band, HV) Supplemented by Optical Data: A Case Study of Biebrza Wetlands in Northeast Poland.” Remote Sensing, vol. 6, 2014, pp. 1605-1633. doi:10.3390/rs6021605.

Dye, Dennis G., et al. “Exploiting differential vegetation phenology for satellite-based mapping of semiarid grass vegetation in the southwestern United States and northern Mexico.” Remote Sensing, vol. 8, no. 11, pp. 889. doi:10.3390/rs8110889

Lee, Christine M. Lee, et al. “An introduction to the NASA Hyperspectral InfraRed Imager (HyspIRI) mission and preparatory activities.” Remote Sensing of Environment, vol. 167, 2015, pp. 6-19. doi:10.1016/j.rse.2015.06.012.

Sankey, Temuulen, et al. “WorldView-2 High Spatial Resolution Improves Desert Invasive Plant Detection.” Photogrammetric Engineering & Remote Sensing, vol. 80, no. 9, September 2014, pp. 885-893. doi:10.14358/PERS.80.9.885.

Van de Ven, C., and S. B. Weiss. “Mapping Arid Vegetation Species Distributions In The White Mountains, Eastern California, Using AVIRIS, Topography, And Geology.” Proceedings of the Tenth JPL Airborne Earth Science Workshop, vol. 10, December 2001, pp. 411-419. ntrs.nasa.gov/search.jsp?R=20020045182

Xie, Yichun, Zongyao Sha, and Mei Yu. “Remote Sensing Imagery in Vegetation Mapping: A Review.” Journal of Plant Ecology, vol. 1, no. 1, March 2008. doi:10.1093/jpe/rtm005.

Remote Sensing of Tamarisk

Evangelista, Paul H., et al. "Mapping invasive tamarisk (*Tamarix*): a comparison of single-scene and time-series analyses of remotely sensed data." Remote Sensing, vol. 1 no. 3, 2009, pp. 519-533. doi:10.3390/rs1030519.

Everitt, J. H., and C. J. Deloach. “Remote Sensing of Chinese Tamarisk and Associated Vegetation.” Weed Science, vol. 38, no. 3, May 1990, pp. 273–278. www.jstor.org/stable/4045024.

Gaskin, John F. “Molecular Systematics and the Control of Invasive Plants: A Case Study of *Tamarix* (Tamaricaceae).” Annals of the Missouri Botanical Garden, vol. 90, no. 1, 2003, pp. 109–118. JSTOR, JSTOR, www.jstor.org/stable/3298530.

Hamada, Yuki, et al. Detecting Tamarisk species (*Tamarix* spp.) in riparian habitats of Southern California using high spatial resolution hyperspectral imagery.” Remote Sensing of Environment, vol. 109, 2007, pp. 237-248. doi:10.1016/j.rse.2007.01.003.

Hurley, A. “Identifying Gypsy Moth Defoliation in Ohio Using Landsat Data.” Environmental & Engineering Geoscience, vol. 10, no. 4, pp. 321-328. doi:10.2113/10.4.321.

Meng, Ryan, et al. “Detection of Tamarisk Defoliation by the Northern Tamarisk Beetle Based on Multispectral Landsat 5 Thematic Mapper Imagery.” GIScience & Remote Sensing, vol. 49, no. 4, 2012, pp. 510-537. doi:10.2747/1548-1603.49.4.510.

West, Amanda M., et al. “Integrating Remote Sensing with Species Distribution Models; Mapping Tamarisk Invasions Using the Software for Assisted Habitat Modeling (SAHM).” Journal of Visualized Experiments : JoVE, no. 116, Oct. 2016. PubMed Central, doi:10.3791/54578.

Invasive Species Detection and Mapping via Remote Sensing

Andrew, Margaret E., and Susan L. Ustin. “The role of environmental context in mapping invasive plants with hyperspectral image data.” *Remote Sensing of Environment,* vol. 112, 2008, pp. 4301-4317. doi:10.1016/j.rse.2008.07.016.

Dennison, Philip E., and Dar A. Roberts. “The effects of vegetation phenology on endmember selection and species mapping in southern California chaparral.” Remote Sensing of Environment, vol. 87, July 2003, pp. 295-309. doi:10.1016/j.rse.2003.07.001.

Dorigo, Wouter, et al. “Mapping Invasive *Fallopia japonica* by Combined Spectral, Spatial, and Temporal Analysis of Digital Orthophotos.” International Journal of Applied Earth Observation and Geoinformation, vol. 19, Oct. 2012, pp. 185–95. doi:10.1016/j.jag.2012.05.004.

Ge, Shaokui, et al. “Estimating Yellow Starthistle (*Centaurea solstitialis*) Leaf Area Index and Aboveground Biomass with the Use of Hyperspectral Data.” Weed Science, vol. 55, no. 6, 2007, pp. 671-678. doi: 10.1614/WS-06-212.1.

Ghulam, Abduwasit, Ingrid Porton, and Karen Freeman. “Detecting subcanopy invasive plant species in tropical rainforest by integrating optical and microwave (InSAR/PolInSAR) remote sensing data, and a decision tree algorithm.” ISPRS Journal of Photogrammetry and Remote Sensing, vol. 88, February 2014, pp. 174-192. doi:10.1016/j.isprsjprs.2013.12.007.

He, Kate S., et al. “Benefits of Hyperspectral Remote Sensing for Tracking Plant Invasions.” Diversity and Distributions, vol. 17, no. 3, May 2011, pp. 381–92. Wiley Online Library, doi:10.1111/j.1472-4642.2011.00761.x.

Hestir, Erin L., et al. “Identification of invasive vegetation using hyperspectral remote sensing in the California Delta ecosystem.” Remote Sensing of Environment, vol. 112, no. 11, 2008, pp. 4034-4047. doi: 10.1016/j.rse.2008.01.022.

Jay, Steven, et al. “Invasive Species Mapping Using Low Cost Hyperspectral Imagery.” *American Society for Photogrammetry and Remote Sensing Annual Conference 2009,* ASPRS 2009. 365-373.

Lass, Lawrence W., et al. “Assessing Agreement in Multispectral Images of Yellow Starthistle (Centaurea solstitialis) with Ground Truth Data Using a Bayesian Methodology.” Weed Technology, vol 14, 2000, pp. 539–544. doi:10.1614/0890-037X(2000)014[0539:AAIMIO]2.0.CO;2.

Lass, Lawrence W., et al. “A review of remote sensing of invasive weeds and example of the early detection of spotted knapweed (*Centaurea maculosa*) and babysbreath (*Gypsophila paniculata*) with a hyperspectral sensor.” Weed Science, vol. 53, no. 2, 2005, pp. 242-251. doi:10.1614/WS-04-044R2.

Lawes, Roger A., and Jeremy F. Wallace. “Monitoring an Invasive Perennial at the Landscape Scale with Remote Sensing.” Ecological Management & Restoration, vol. 9, no. 1, Apr. 2008, pp. 53–59. Wiley Online Library, doi:10.1111/j.1442-8903.2008.00387.x.

Lawrence, Rick L., et al. “Mapping Invasive Plants Using Hyperspectral Imagery and Breiman Cutler Classifications (randomForest).” *Remote Sensing of Environment*, vol. 100, no. 3, Feb. 2006, pp. 356–62. *ScienceDirect*, doi:10.1016/j.rse.2005.10.014.

Müllerová, Jana, Jan Pergl, and Petr Pyšek. “Remote sensing as a tool for monitoring plant invasions: Testing the effects of data resolution and image classification approach on the detection of a model plant species *Heracleum mantegazzianum* (giant hogweed).” International Journal of Applied Earth Observation and Geoinformation, vol. 25, December 2013, pp. 55-65. doi:10.1016/j.jag.2013.03.004.

Narumalani, Sunil, et al. “Detecting and Mapping Four Invasive Species along the Floodplain of North Platte River, Nebraska.” Weed Technology, vol. 23, no. 1, January 2009, pp. 99-107. doi: 10.1614/WT-08-007.1.

Nguyen, Andrew, et al. “Hyperspectral Mapping of the Invasive Species Pepperweed and the Development of a Habitat Suitability Model.” ASPRS 2012: proceedings of the Annual ASPRS Conference, 19-23 March 2012, Sacramento, California. https://www.asprs.org/Conference-Proceedings.html.

Rogan, John, Janet Franklin, and Dar A. Roberts. “A Comparison of Methods for Monitoring Multitemporal Vegetation Change Using Thematic Mapper Imagery.” Remote Sensing of Environment, vol. 80, no. 1, Apr. 2002, pp. 143–56. ScienceDirect, doi:10.1016/S0034-4257(01)00296-6.

Roth, Keely L., et al. “Differentiating Plant Species within and across Diverse Ecosystems with Imaging Spectroscopy.” Remote Sensing of Environment, vol. 167, Sept. 2015, pp. 135–51. ScienceDirect, doi:10.1016/j.rse.2015.05.007.

Skowronek, Sandra, Gregory P. Asner, and Hannes Feilhauer. “Performance of one-class classifiers for invasive species mapping using airborne imaging spectroscopy.” Ecological Informatics, vol. 37, Jan 2017, pp. 66-76. doi:10.1016/j.ecoinf.2016.11.005.

Ustin, Susan L., et al. “Using Imaging Spectroscopy to Study Ecosystem Processes and Properties.” BioScience, vol. 54, no. 6, June 2004, pp. 523–534. doi:10.1641/0006-3568(2004)054[0523:UISTSE]2.0.CO;2

Ustin, Susan L., and John A. Gamon. “Remote sensing of plant functional types.” New Phytologist, vol. 186, no. 4, May 2010, pp. 795–816. doi: 10.1111/j.1469-8137.2010.03284.x.

Vanderhoof, Melanie, et al. “Predicting the Distribution of Perennial Pepperweed (Lepidium Latifolium), San Francisco Bay Area, California.” Invasive Plant Science and Management, vol. 2, no. 3, July 2009, pp. 260–69. doi:10.1614/IPSM-09-005.1.

Wang, Yachao, and Gang Wu. “Plant Species Identification Based on Independent Component Analysis for Hyperspectral Data.” Journal of Software, vol. 9, no. 6, June 2014, pp. 1532-1537. doi:10.4304/jsw.9.6.1532-1537.

Yano, Inacio H., et al. “Identification of weeds in sugarcane fields through images taken by UAV and Random Forest classifier.” IFAC-PapersOnLine, vol. 49, no. 16, 2016, pp. 415-420. doi:10.1016/j.ifacol.2016.10.076.

Zhang, Caiyun, and Zhixiao Xie. “Combining object-based texture measures with a neural network for vegetation mapping in the Everglades from hyperspectral imagery.” Remote Sensing of Environment., vol. 124, pp. 310-320. doi: 10.1016/j.rse.2012.05.015.

Invasive Plant Species of California

Blackburn WH, Knight RW, Schuster JL. 1982. Saltcedar influence on sedimentation in the Brazos River. Journal of Soil and Water Conservation 37:298-301.

Busch DE. 1995. Effects of fire on southwestern riparian plant community structure. The Southwestern Naturalist 40:259-267.

Busch DE, Smith SD. 1995. Mechanisms associated with decline of woody species in riparian ecosystems of the southwestern U.S. Ecological Monographs 65:347-370.

“Gateway to Invasive Species Information; Covering Federal, State, Local, and International Sources.” National Invasive Species Information Center, United States Department of Agriculture, National Agriculture Library, 24 Jan. 2018, www.invasivespeciesinfo.gov/index.shtml.

U.S. Fish and Wildlife Service. “Listed Species Believed to or Known to Occur in California.” Listed Species Believed to or Known to Occur in California, US Fish & Wildlife Service, 13 Feb. 2015, ecos.fws.gov/ecp0/reports/species-listed-by-state-report?state=CA&status=listed.

Vegetation Ecology Mapping & Management

Dirr, Michael A. (1997), Dirr's Hardy Trees and Shrubs, an illustrated encyclopedia, p. 392.

DiTomaso, J.M, G. B. Kyser, and M. J. Pitcairn. 2006. “Yellow starthistle management guide.” Cal-IPC Publication 2006-03. California Invasive Plant Council: Berkeley, CA. 78 pp. Available: www.cal-ipc.org.

Hobbs, Richard J., and Stella E. Humphries. "An integrated approach to the ecology and management of plant invasions." Conservation Biology 9.4 (1995): 761-770.

https://www.amnh.org/explore/science-bulletins/bio/documentaries/species-and-sprawl-a-road-runs-through-it/species-and-sprawl-yellow-starthistle/

The Nature Conservancy. (1994), Field Methods for Vegetation Mapping: USGS/NPS Vegetation Mapping Program.

Vos, P., E. Meelis, and W. J. Ter Keurs. "A framework for the design of ecological monitoring programs as a tool for environmental and nature management." *Environmental monitoring and assessment* 61.3 (2000): 317-344.

Cost-Benefit Analysis of Monitoring

Gardner, T. A., *et al.* (2008), The cost-effectiveness of biodiversity surveys in tropical forests. Ecology Letters, 11: 139–150. doi:10.1111/j.1461-0248.2007.01133.x

Lingane, Alison, and Sara Olsen. "Guidelines for social return on investment." California management review 46.3 (2004): 116-135.

Species Distribution Modeling & Adaptive Management

Abella, Scott R. Jessica E. Spencer, Josh Hoines, and Carrie Nazarchyk. “Assessing an exotic plant surveying program in the Mojave Desert, Clark County, Nevada, USA.” *Environmental monitoring and assessment*, vol. 151, 2008, pp. 221-30. doi:10.1007/s10661-008-0263-0.

Burton, Cole, et al. “A framework for adaptive monitoring of the cumulative effects of human footprint on biodiversity.” *Environmental monitoring and assessment*, vol. 186, 2014. doi:10.1007/s10661-014-3643-7.

Davies, Kirk W., and Roger L. Sheley. “A Conceptual Framework for Preventing the Spatial Dispersal of Invasive Plants.” Weed Science, vol. 55, no. 02, 2007, pp. 178–184. doi:10.1614/ws-06-161.

Herring, Carlie E., Jonah Stinson, and Wayne G Landis. “Evaluating nonindigenous species management in a Bayesian networks derived relative risk framework for Padilla Bay, WA, USA.” *Integrated Environmental Assessment and Management* , vol. 11, no. 4, 2015, pp. 640-652. doi:10.1002/ieam.1643.

Fourcade, Yoan et al. “Mapping Species Distributions with MAXENT Using a Geographically Biased Sample of Presence Data: A Performance Assessment of Methods for Correcting Sampling Bias.” Ed. John F. Valentine. PLoS ONE, vol. 9, no. 5, 2014. doi:10.1371/journal.pone.0097122.

Hoffman, Justin D., et al. “Predicting Potential Occurrence and Spread of Invasive Plant Species along the North Platte River, Nebraska. “Invasive Plant Science and Management, vol. 1, no. 04, Oct. 2008, pp. 359–367., doi:10.1614/ipsm-07-048.1.

Howes, Alison L., Martine Maron, and Clive A. Mcalpine. “Bayesian Networks and Adaptive Management of Wildlife Habitat.” *Conservation Biology*, vol. 24, no. 4, 2010, pp. 974-983. doi: 10.1111/j.1523-1739.2010.01451.x.

International Society for Photogrammetry and Remote Sensing. www.itc.nl/library/Papers_2004/peer_conf/joshi.pdf.

Joshi, Chudamani, Jan De Leeuw, and Iris Van Duren. “Remote sensing and GIS applications for mapping and spatial modeling of invasive species.” ISPRS 2004: proceedings of the XXth ISPRS congress: Geo-imagery bridging continents, 12-23 July 2004, Istanbul, Turkey. Comm. vol. 7. pp. 669-677. Istanbul, Turkey:

Lindenmayer, David B., and Gene E. Likens. “The science and application of ecological monitoring.” *Biological Conservation,* vol. 143, 2010, pp. 1317-1328. doi:10.1016/j.biocon.2010.02.013.

Merow, Cory, et al. “A practical guide to MaxEnt for modeling species’ distributions: what it does, and why inputs and settings matter.”Ecography, vol. 36, no. 10, 2013, pp. 1058–1069., doi:10.1111/j.1600-0587.2013.07872.x.

Phillips, Steven J., et al. “A maximum entropy approach to species distribution modeling.” Twenty-First international conference on Machine learning - ICML 04, 2004, doi:10.1145/1015330.1015412.

Sánchez-Flores, E, H. Rodríguez-Gallegos, and S. R. Yool. “Plant invasions in dynamic desert landscapes. A field and remote sensing assessment of predictive and change modeling.” Journal of Arid Environments, vol. 72, no. 3, March 2008, pp. 189-206. doi:10.1016/j.jaridenv.2007.05.013.

2014 California BCM (Basin Characterization Model) Downscaled Climate and Hydrology - 30-Year Summaries.” *2014 California BCM (Basin Characterization Model) Downscaled Climate and Hydrology - 30-Year Summaries | California Climate Commons*, California Landscape Conservation Cooperative, climate.calcommons.org/node/1129.

Object-Based Image Analysis and Classification Using Texture

Blaschke, T. “Object based image analysis for remote sensing.” *ISPRS Journal of Photogrammetry and Remote Sensing*, vol. 65, no. 1, 2010, pp. 2-16. doi:10.1016/j.isprsjprs.2009.06.004.

Feng, Quanlong, Jiantao Liu, and Jianhua Gong. “UAV Remote Sensing for Urban Vegetation Mapping Using Random Forest and Texture Analysis.” *Remote Sensing,* vol. 7, 2015, pp. 1074-1094. doi:10.3390/rs70101074.

Heurich, Marco, Tobias Ochs, Thorsten Andresen, and Thomas Schneider. “Object-orientated image analysis for the semi-automatic detection of dead trees following a spruce bark beetle (*Ips typographus*) outbreak.” *European Journal of Forest Research,* vol. 129, 2010, pp. 313-324. doi:10.1007/s10342-009-0331-1.

Hung, Calvin, Zhe Xu, and Salah Sukkarieh. “Feature Learning Based Approach for Weed Classification Using High Resolution Aerial Images from a Digital Camera Mounted on a UAV.” *Remote Sensing,* vol. 6, 2014, pp. 12037-12054. doi:10.3390/rs61212037.

Laliberte, Andrea S., and Al Rango. “Incorporation of Texture, Intensity, Hue, and Saturation for Rangeland Monitoring with Unmanned Aircraft Imagery.” *The Jornada Foundation Publications,* 2008. https://jornada.nmsu.edu/bibliography/08-046.pdf.

Ryherd, Soren, and Curtis Woodcock. “Combining spectral and texture data in the segmentation of remotely sensed images.” *Photogrammetric Engineering and Remote Sensing*, vol. 41, 1996.

Schiewe, Jochen**.** “Segmentation of High-resolution Remotely Sensed Data - Concepts, Applications and Problems.” *International Archives of Photogrammetry and Remote Sensing,* 2002.

Szantoi, Zoltan, Francisco Escobedo, Amr Abd-Elrahman, Scot Smith, and Leonard Pearlstine. “Analyzing fine-scale wetland composition using high resolution imagery and texture features.” *International Journal of Applied Earth Observation and Geoinformation*, vol. 23, 2013, pp. 204-212. doi:10.1016/j.jag.2013.01.003.

Tejon Ranch Conservancy Documents

“Ranch-Wide Management Plan.” Tejon Ranch Conservancy's Ranch-Wide Management Plan, Tejon Ranch Company and Tejon Ranch Conservancy, 2008, www.tejonconservancy.org/rwmp.htm.